TRITA-EPP-78-16

ELECTRON TEMPERATURE MEASUREMENTS IN LOW DENSITY PLASMAS BY HELIUM SPECTROSCOPY II - PARAMETER LIMITS FOR VALIDITY OF DIFFERENT METHODS

Nils Brenning

December 1978

Department of Plasma Physics
Royal Institute of Technology
S-100 44 Stockholm 70 Sweden

ELECTRON TEMPERATURE MEASUREMENTS IN LOW DENSITY PLASMAS BY HELIUM SPECTROSCOPY II - PARAMETER LIMITS FOR VALIDITY OF DIFFERENT METHODS

N. Brenning
Royal Institute of Technology, Department of Plasma Physics,
S-100 44 Stockholm, Sweden

Abstract

Different methods to measure electron temperature in low-density plasmas by He spectroscopy are examined. They are based either on the relative intensities of singlet and triplet lines or on the absolute intensities of single lines. Calculations from measured and theoretical data show that both methods are seriously influenced by secondary processes, the dominating being excitation from the metastable levels 2^1S and 2^3S, and excitation transfer in electron-atom collisions combined with imprisonment of resonance radiation. The calculations give parameter limits for validity of different methods and combinations of lines. Due to the secondary processes, T_e-determination from relative line intensities is limited to low-density, short-duration plasmas (typically $n_e < 2 \cdot 10^{16} m^{-3}$, $t_{ex} < 5 \cdot 10^{-6} s$) or to even lower densities that depend on the apparatus dimensions (typically $n_e < 3 \cdot 10^{15} m^{-3}$, $L \approx 0.1$ m).

For T_e-determination from absolute line intensities the situation is more favourable, and with a suitable choise of lines the restrictions on n_e and t_{ex} can be typically ($n_e < 5 \cdot 10^{17} m^{-3}$, $t_{ex} < 10^{-5} s$) or ($n_e < 10^{17} m^{-3}$, $L \approx 0.1$ m) for electron temperatures above 10 eV. For temperatures below 10 eV and degrees of imprisonment below 7% measurements are possible for electron densities up to 10^{19} or $10^{20} m^{-3}$, and without any limits on t_{ex} or L.

1. INTRODUCTION

1.1 Background

One method to measure electron temperature in plasmas is based on the relative intensities of neutral helium lines. Since it was first proposed by Cunningham (1954), this method has been in common use. Developments of the method have been made by for example Sovie (1964) and Eastlund et al. (1973). However, there have been warnings against the effects of secondary processes in a plasma which could influence the helium line intensities and invalidate the method (Drawin 1964, 1967; de Vries and Mewe 1965; Mewe 1967).

The present work is an examination of such processes that are important for the intensities of lines originating in the HeI levels 3^1P, 4^1S, 5^1S, 4^1D, 5^1D, 3^3P, 4^3S, 5^3S, 4^3D and 5^3D at low electron densities (below $10^{18} m^{-3}$). The aim is to determine limiting values of relevant parameters (such as plasma density, electron temperature and duration of an experiment) for the applicability of the diagnostic method. These limits turn out to vary rather much with the specific choice of lines and evaluation method. Earlier estimates of for example upper limits of n_e vary from author to author (Eastlund et al. (1973), Sovie (1964), de Vries and Mewe (1966), Mewe (1967)), but they are generally optimistic with a factor of 10 to 100 compared to the results in the present work.
T_e-determination based on the absolute line intensities is possible in a wider parameter range, but experimentally somewhat more complicated than the method based on relative line intensities. This method is discussed in Section 6 below.

Some of the results are already published in an preliminary report (Brenning 1977), but included here for the sake of completeness.

1.2 Outline of the calculations

Electron temperature determination as proposed by Cunningham is based on the fact that the dependence on the electron energy of the cross sections for excitation by electron impact differs widely between singlet and triplet lines of neutral helium. The electron temperature in an experiment is calculated from measured line intensities by the use of excitation cross sections, obtained in collision chamber experiments. It is assumed that line emission is

the result of single collisions between electrons and helium atoms in the ground state followed by direct radiative de-excitation. This assumption may be false in a plasma due to a number of secondary processes involving collisions with the plasma electrons. Some processes can be disregarded if the density is low enough. When the electron density is below $10^{20} m^{-3}$ volume recombination is unimportant (de Vries and Mewe 1966) and when the density of He in the ground state is below $10^{20} m^{-3}$, excitation transfer in He-He collisions can be neglected (Lin and St John 1962; Kay and Hughes 1967). This leaves the following processes involving collisions between electrons and neutral He atoms:

i) Excitation from metastables
The upper line levels can be excited through collisions between electrons and He atoms in the metastable levels 2^1S and 2^3S.

ii) Excitation transfer collisions
The upper line levels can be populated or depopulated by excitation transfer collisions with electrons before radiative de-excitation.

iii) Redistribution of cascading
Part of the single-collision excitation of a line is excitation to a high-lying level, followed by cascading to the upper level of the line in question. Excitation transfer and ionization among the high-lying levels influence the cascading process.

These three groups of processes are studied separately in Sections 2, 3 and 4 below. A summary of the results and a discussion of the consequences for T_e-determination by Cunningham's method follows in Section 5. In Section 6, the possibility to determine T_e from the absolute intensities of single lines is discussed.

1.3 The apparent rate coefficient S_λ^*

We will need a quantity that conveniently shows the effect of secondary processes. For this purpose S_λ^* and S_λ are introduced.

S_λ^* is the "apparent excitation rate coefficient" for excitation of the line with wavelength λ from the ground state, with all secondary processes included. The line emission in photons $m^{-3}s^{-1}$ is then:

$$N_\lambda = n_e n_{He(1^1S)} S_\lambda^* \qquad (1)$$

S_λ^* is a function of the electron density and temperature, the degree of imprisonment of resonance radiation, and the population densities of the metastable levels (which again depend on a number of parameters).

S_λ is the corresponding line excitation rate coefficient for single collision excitations, when all secondary collisional processes can be disregarded. S_λ is a function only of the electron temperature T_e.

In the following sections, we will calculate the quantity S^*_λ/S_λ, which is the factor by which the line intensitites are changed by the secondary processes considered.

The aim of this work is to establish for what n_e, T_e etc. any secondary process will influence the line intensitites so much that T_e-determination becomes uncertain. Each process is therefore treated under the assumption that the line intensities are uninfluenced by other processes. No attempt has been made to calculate the combined effect when many secondary processes operate at the same time. However, a rough estimate of the "combined S^*_λ/S_λ" can be obtained by multiplication of the individual S^*_λ/S_λ values for the different processes. This "combined S^*_λ/S_λ" becomes increasingly uncertain as more than one of the indicidual S^*_λ/S_λ values depart from one.

1.4 Presentation of the results

Figures 3a-3d and Tables I-IV gives S^*_λ/S_λ values for ten lines and a wide range of experimental parameters. These values can be used in combination with the S_λ (T_e) values in Fig. 5 to determine the errors in T_e determination due to each secondary process.

For a determination of whether a line is suitable or not for T_e-determination in a particular experiment, Tables V-VII are recommended. Table V gives limits to experimental parameters corresponding to the requirement that T_e-determination from the singlet-to-triplet intensity ratio shall be uncertain by less than a factor 1.5 (either way). Tables VI and VII give the same information for T_e-determination from absolute line intensities and uncertainty factors less than 1.1, 1.2 or 1.5.

1.5 Lines with longer wavelength

The HeI lines originating in the n = 3 levels 7281 Å ($3^1S - 2^1P$), 6678 Å ($3^1D - 2^1P$), 7056 Å ($3^3S - 2^3P$) and 5876 å ($3^3D - 2^3P$) are in some respects more favourable for T_e-determination than the lines originating in the n = 4 levels. The cross sections are typically a factor of 2-3 larger, and the lines are less influenced by excitation transfer. On the other hand, the lines from n = 3 are more influenced than the lines from n = 4 by excitations from the metastable levels. The use of these lines therefore only

gives a small advantage in plasmas of very low density or short duration, where the metastable population is low. Furthermore, the lines originating in n = 3 are not among those that earlier have been recommended for T_e-determination. The calculations have therefore not been extended to cover these lines.

2. EXCITATION FROM THE METASTABLE LEVELS

When excitation of the upper line levels through collisions between electrons and atoms in the metastable levels 2^1S and 2^3S is the only secondary process in operation, the quantity S^*_λ/S_λ is:

$$\frac{S^*_\lambda}{S_\lambda} = \frac{N_{1^1S\to j} + N_{2^1S\to j} + N_{2^3S\to j}}{N_{1^1S\to j}} \qquad (2)$$

where $N_{1^1S\to j}$ etc. are the excitation rates in excitations $m^{-3}s^{-1}$ to the upper line level j. The excitation rates are given by

$$N_{1^1S\to j} = n_e\, n_{1^1S}\, S_{1^1S\to j} \qquad (3)$$

$$N_{2^1S\to j} = n_e\, n_{2^1S}\, S_{2^1S\to j} \qquad (4)$$

$$N_{3^3S\to j} = n_e\, n_{2^3S}\, S_{2^3S\to j} \qquad (5)$$

The population densitites n_{2^1S} and n_{2^3S} in (4) and (5) are characterized by a relaxation time t_r for build-up of an equilibrium population. t_r is a function of n_e, T_e and the degree I of imprisonment of resonance radiation. Table I gives the "reduced relaxation time" $n_e t_r$ for 2^1S and 2^3S as calculated in appendix I.1.4.

2.1 Excitations from equilibrium population of metastables

In equilibrium, when t_r is much shorter than both the experimental time t_{ex} and the time t_{diff} it takes a metastable atom to diffuse out of the laboratory plasma, the metastable population densitites are coupled to the ground-state density by the rate equations:

$$n_e\, n_{2^1S}\, \Sigma^2\, S_{2^1S\to i,\, 1^1S} = n_e\, n_{1^1S}\, \Sigma^1\, S_{1^1S\to 2^1S} \qquad (6)$$

$$n_e\, n_{2^3S}\, \Sigma^2\, S_{2^3S\to i,\, 1^1S} = n_e\, n_{1^1S}\, \Sigma^1\, S_{1^1S\to 2^3S} \qquad (7)$$

$\Sigma^1\, S_{1^1S\to 2^1S}$ and $\Sigma^1\, S_{1^1S\to 2^3S}$ are the sums of the rate coefficients $S = \langle \sigma v_e \rangle$ for all routes of excitation from the ground state to the metastable levels 2^1S and 2^3S.

$\Sigma^2\, S_{2^1S\to i,\, 1^1S}$ and $\Sigma^2\, S_{2^3S\to i,\, 1^1S}$ are the sums of the rate coefficients for all routes of de-excitation from 2^1S and 2^3S, sometimes via other excited states, leading either to ionization or to an atom in the ground state.

Equations (2) - (7) can be combined to give S^*_λ/S_λ for equilibrium population of metastables:

$$\left(\frac{S^*_\lambda}{S_\lambda}\right)_{\text{eq.met.}} = 1 + \frac{1}{S_{1^1S\to j}}\left(\frac{\Sigma^1\, S_{1^1S\to 2^1S}}{\Sigma^2\, S_{2^1S\to i,1^1S}}\, S_{2^1S\to j} + \frac{\Sigma^1\, S_{1^1S\to 2^3S}}{\Sigma^2\, S_{2^3S\to i,1^1S}}\, S_{2^3S\to j}\right) \qquad (8)$$

It is worth noting that neither n_e nor n_{He} enter explicitly into (8). However, there is some variation with n_{He} implicit in $\Sigma^1\, S_{1^1S\to 2^1S}$ and $\Sigma^2\, S_{2^1S\to i,\, 1^1S}$ since these sums are functions of the degree of imprisonment I of resonance radiation, which depends on n_{He}. The rate coefficients needed to solve (8) were calculated from measured and theoretical cross sections as described in Appendix I.

With these rate coefficients, equation (8) has been solved for eight HeI lines, for electron temperatures between 5 and 200 eV [1eV = 7740 K] and for degrees of imprisonment $0\% < I < 50\%$. The results are tabulated in Tables II and III. The uncertainties arise from uncertainties in the rate coefficients.

Table II is divided in two parts, excitations $2^1S\to$ singlet levels and excitations $2^3S\to$ singlet levels. The reason for this is that no reliable estimates of cross sections exist for the latter processes, which involve change in multiplicity. Such excitations can only occur in electron exchange collisions. The cross sections are therefore probably smaller than the corresponding cross sections for unchanged multiplicity, which include both exchange and non-exchange collisions (for example $\sigma_{2^3S\to 4^1D} < \sigma_{2^3S\to 4^3D}$). This assumption applied to equation (8) gives the upper limits on S^*_λ/S_λ given in Table IIb.

2.2 Excitation from a non-equilibrium population of metastables

Either the time t_{diff} it takes a metastable atom to diffuse out of the laboratory plasma or the experimental time t_{ex} can be smaller than the relaxation time t_r for build-up of equilibrium population of metastables. Then the metastable population n_m is approximately:

$$n_m \approx n_{m(equilibrium)} \min\left\{\frac{t_{diff}}{t_r}, \frac{t_{ex}}{t_r}\right\} \qquad (9)$$

where $\min\left\{t_{diff}/t_r, t_{ex}/t_r\right\}$ represents the smallest of t_{diff}/t_r and t_{ex}/t_r. The S^*_λ/S_λ values can then be approximately calculated from the equilibirum values in tables II and III:

$$\frac{S^*_\lambda}{S_\lambda} \approx 1 + \min\left\{\frac{t_{diff}}{t_r}, \frac{t_{ex}}{t_r}\right\}\left(\left(\frac{S^*_\lambda}{S_\lambda}\right)_{eq.met.} - 1\right) \qquad (10)$$

3. EXCITATION TRANSFER COLLISIONS

Excitation transfer collisions between electrons and He atoms in the upper line levels can occur during the natural lifetimes of the levels. Optically allowed transitions between levels with the same main quantum number have the largest cross sections and will operate at the lowest plasma densities. These transitions are illustrated by arrows in Fig. 1. When this is the only secondary process of importance, the values of S^*_λ/S_λ for each line is determined by the processes illustrated in Fig. 2. The excitations to a group of levels with common main and spin quantum number (for example 4^1D, 4^1P, 4^1D and 4^1F) are redistributed within this group during the natural lifetimes of the levels. The individual levels are populated through excitation from the ground state, cascading, absorption of resonance radiation and excitation transfer from neighbouring levels. They are depopulated through spontaneous radiative transitions and excitation transfer. For each value of the main quantum number, the coupled rate equations for these processes can be written:

$$\begin{pmatrix} A_{11} & A_{12} & 0 & 0 & 0 \\ A_{21} & A_{22} & A_{23} & 0 & 0 \\ 0 & A_{32} & A_{33} & A_{34} & 0 \\ 0 & 0 & A_{43} & A_{44} & A_{45} \\ 0 & 0 & 0 & A_{54} & A_{55} \end{pmatrix} \begin{pmatrix} n_S \\ n_P \\ n_D \\ n_F \\ n_G \end{pmatrix} = n_{1^1S} \begin{pmatrix} B_1 \\ B_2 \\ B_3 \\ B_4 \\ B_5 \end{pmatrix} \qquad (11)$$

where

$A_{11} = -1/n_e \tau_S - S_{S\to P}$ $\quad A_{12} = S_{P\to S} = S_{S\to P}/3 = A_{21}/3$

$A_{21} = S_{S\to P}$ $\quad A_{22} = -S_{S\to P}/3 - S_{P\to D} - 1/n_e \tau_P$

$A_{23} = S_{P\to D} \cdot 3/5 = 3 A_{32}/5$ $\quad A_{32} = S_{P\to D}$

$A_{33} = -S_{P\to D}\ 3/5 - S_{D\to F} - 1/n_e \tau_D$ $\quad A_{34} = S_{D\to F} \cdot 5/7 = A_{43} \cdot 5/7$

$A_{43} = S_{D\to F}$ $\quad A_{44} = -S_{D\to F} \cdot 5/7 - S_{F\to G} - 1/\tau_F n_e$

$A_{45} = S_{F\to G} \cdot 7/9 = A_{54} \cdot 7/9$ $\quad A_{54} = S_{F\to G}$

$A_{55} = -S_{F\to G} \cdot 7/9 - 1/n_e \tau_G$ $\quad B_1 = S_{1^1S\to S}$

$B_2 = S_{1^1S\to P}$ $\quad B_3 = S_{1^1S\to D}$

$B_4 = S_{1^1S\to F}$ $\quad B_5 = S_{1^1S\to G}$

with the following notations:

- n_j is the number density of level j.
- S, P, D, F and G denote levels with azimuthal quantum numbers 0, 1, 2, 3 and 4 within a group of levels with common main and spin quantum numbers.
- $S_{1^1S\to k}$ is the excitation rate from the ground state to the level k, with the cascading process included. (It is here assumed that the cascading contribution can be represented as a constant fraction of the excitations to each level. This is not strictly true (Section 4). However, this simplification influences the results in this section only marginally, while the calculations are simplified considerably).
- $S_{S\to P}$, S_{P-D} etc. are the rate coefficients for excitation transfer. For the reversed processes, the rate coefficients ($S_{P\to S}$, $S_{D\to P}$ etc.) are obtained with use of the principle of

detailed balancing. With g_j denoting the statistical weight of level j, this gives:

$$S_{P\to S} = S_{S\to P}\, g_S/g_P = S_{S\to P} \cdot 1/3$$
$$S_{D\to P} = S_{P\to D}\, g_P/g_D = S_{S\to P} \cdot 3/5$$
$$S_{F\to D} = S_{D\to F}\, g_D/g_F = S_{D\to F} \cdot 5/7$$
$$S_{G\to F} = S_{F\to G}\, g_F/g_D = S_{F\to G} \cdot 7/9$$

which is used in Eq. (11) above.

· τ_j is the natural lifetime of the level j.

For the singlet P levels, the effect of imprisonment of resonance ($n^1P - 1^1S$) radiation is taken into account by replacing τ_P in Equation (11) with the apparent lifetime τ_P^*, which is coupled to the degree of imprisonment. τ_P^* is defined in Appendix II, which also describes the choise of transition probabilities, lifetimes and cross sections in Equation (11).

Eq. (11) has been solved for the population densitites n_j of the levels 4^1S, 5^1S, 4^1D, 5^1D, 4^3S, 5^3S, 4^3D and 5^3D for electron densitites $10^{15} m^{-3} \leq n_e \leq 10^{19}\ m^{-3}$, degrees of imprisonment $0\% \leq I \leq 100\%$, and electron temperatures $5\ eV \leq T_e \leq 100\ eV$. The results are summarized as S_λ^*/S_λ values for the excitation transfer process in Fig. 3 a-d.

The model in Fig. 2 is only valid, when the probability is small for a collisional transition involving a change in main quantum number during the natural lifetime of a level. This condition is fulfilled at different electron densitites for different levels. The curves in Fig. 3 are dotted where the results are uncertain due to this effect.

The effect of the excitation transfer process is that the intensitites of lines with S levels as upper levels decrease with increasing n_e, while the intensitites of lines originating in D levels increase or remain constant. This is expected, since the excitations are redistributed from S levels towards D levels with their greater statistical weight. In the high-density limit, the relative population of levels with the same main quantum number is determined only by their statistical weight. This could be seen as a "horizontal thermal equilibrium" between those levels.

4. REDISTRIBUTION OF CASCADING

4.1 Model

Part of the single-collision excitation of a line is excitation to a high-lying level, followed by cascading to the upper level of the line in question. Excitation transfer and ionization among the high-lying levels influence the cascading. Due to the great number of levels involved in this process, a simplified model is necessary for the calculation of S^*_λ/S_λ. We use the fact that the cross sections for both the secondary processes (ionization and excitation transfer) increase with increasing main quantum number approximately as n^4 (Appendix II.1), while the lifetimes increase approximately as n^3 (Appendix III.1.4). This means that the number of collisions during a natural lifetime changes very rapidly with n (roughly as n^7). For a given value of n, each of the secondary processes can therefore be approximated to be either negligible or dominating for the level populations.

In this model the levels are divided into three groups according to their main quantum number n:

Group I. $n \leq n_1$. Both excitation transfer and ionization are negligible.

Group II. $n_1 < n \leq n_2$. Excitation transfer is assumed to determine the level populations, and the ionization time is longer than the natural lifetime.

Group III. $n > n_2$. The ionization time is shorter than the natural lifetime. This means that excitations to group III will give no contribution to the cascading to lower-lying levels.

The determination of n_1 and n_2 as functions of the electron density is described in Appendix III.1. The result is summarized in Fig. 4.

The cascading from each group is calculated below.

4.2 Calculations

4.2.1. Cascading from levels in Group I.

When both excitation transfer and ionization can be neglected, the cascading to the level j from the level r in excitations $m^{-3}s^{-1}$ is

$$N_{r\to j} = n_e \, n_{1^1S} \, S'_{1^1S\to r}/B_{r\to j} \qquad (12)$$

The sign $S'_{S^1S\to r}$ denotes that cascading is not included in the excitation rate coefficient (see Appendix I.1.1).

$B_{j\to k}$ is given by equation (I). A summation over r gives the cascading from group I to j:

$$N_{(\text{Group I}\to j)} = n_e\, n_{1^1S} \sum_{n_j < n_r < n_1} \frac{S_{1^1S\to r}\, A_{r\to j}}{\sum_{n_k < n_r} A_{r\to k}} \qquad (13)$$

4.2.2. Cascading from levels in group II.

In this group ionization can be neglected, but excitation transfer dominates the level populations. We assume that the redistribution of the pupulation between levels with the same main quantum number leads to a "horizontal thermal equilibrium", where the levels are populated according to their statistical weights. For the medium energy levels discussed in Section 3 this only meant a redistribution between levels with the same main and spin quantum number. For the high-lying levels, however, this includes a redistribution between the singlet and the triplet system for the following reason: For F levels with $n > 5$, there is no clear distinction between the singlet and the triplet system, since the coupling between the spin vector and the orbital motion of the excited electron becomes greater than the spin-spin coupling between the electrons (Lin and Fowler 1961). Kay and Hughes (1967) have shown experimentally that the cascading from these mixed levels is shared between the singlet and the triplet system as 1:3, which corresponds to the ratio of the statistical weights of the levels n^1F and n^3F.

The total number of excitations to a group of levels with the same main quantum number n_p is:

$$N'_{1^1S\to(\text{all levels with } n = n_p)} = n_e\, n_{1^1S} \sum_{\text{all } \ell \text{ with } n_\ell = n_p} S_{1^1S\to\ell} \qquad (14)$$

(The sign $N'_{1^1S\to(\ )}$ denotes that cascading is not included in the excitation from the ground state (see Appendix I.1.1).)

The fraction of those excitations that goes to transitions r→j is, since the statistical weight of the level r is $(2\ell_r + 1)(2s_r + 1)$,

$$\frac{(2\ell_r + 1)(2s_r + 1)\, A_{r\to j}}{\sum_{\left[\begin{smallmatrix}\text{all m with}\\ n_m = n_p\end{smallmatrix}\right]} \sum_{\left[\begin{smallmatrix}\text{all k with}\\ n_k < n_m\end{smallmatrix}\right]} (2\ell_m + 1)(2s_m + 1)\, A_{m\to k}} \tag{15}$$

ℓ_r is the azimuthal and s_r the spin quantum number of the level r. A summation now gives the number of excitations to the level j from group II.

(16)

$$N_{(\text{group two}\to j)} = n_e\, n_{1^1S} \frac{\sum_{\left[\begin{smallmatrix}\text{all } \ell \text{ with}\\ n_\ell = n_p\end{smallmatrix}\right]} S'_{1^1S\to\ell} \sum_{\left[\begin{smallmatrix}\text{all r with}\\ n_r = n_p\end{smallmatrix}\right]} (2\ell_r + 1)(2s_r + 1) A_{r\to j}}{\sum_{\left[\begin{smallmatrix}\text{all } n_p \text{ with}\\ n_1 < n_p \le n_2\end{smallmatrix}\right]} \sum_{\left[\begin{smallmatrix}\text{all m with}\\ n_m = n_p\end{smallmatrix}\right]} \sum_{\left[\begin{smallmatrix}\text{all k with}\\ n_k < n_m\end{smallmatrix}\right]} (2\ell_m + 1)(2s_m + 1) A_{m\to k}}$$

4.2.3. Cascading from levels in group III.

Excitations to this group gives no contribution to the cascading to lower-lying levels.

4.2.4. Calculation of S^*_λ / S_λ due to the cascading.

The total number of excitations to level j is, with the use of Equations (1) and (I):

$$N_{(\text{group one})\to j} + N_{(\text{group two})\to j} + N'_{1^1S\to j} = n_e\, n_{1^1S}\, S^*_\lambda\, B_\lambda \tag{17}$$

S_λ is given by

$$N_{1^1S\to j} = N'_{1^1S\to j} + N'_{(\text{group one with } n_1 = \infty)\to j} = n_e\, n_{1^1S}\, S_\lambda\, B_\lambda \tag{18}$$

(14) and (15) give:

$$\frac{S^*_\lambda}{S_\lambda} = \frac{N_{(\text{group one})\to j} + N_{(\text{group two})\to j} + N'_{1^1S\to j}}{N_{(\text{group one with } n_1 = \infty)\to j} + N'_{1^1S\to j}} \qquad (19)$$

This is solved with the use of Equations (13) and (16).

Imprisonment of resonance radiation is taken into account by replacing the $A_{n^1p\to 1^1S}$ transition probabilities with the apparent transition probabilities $A^*_{n^1p\to 1^1S}(I)$ (Appendix II.3). The choise of transition probabilities and cross sections needed to solve (19) is discussed in Appendix III.2.

S^*_λ/S_λ for the cascading redistribution has been calculated from Equation (19) for eight helium lines, for electron densities $10^{14}m^{-3} < n_e < 10^{17}m^{-3}$, and for zero and complete imprisonment. (For $n_e > 10^{17}m^{-3}$, the excitation transfer process dominates compared to the redistribution of cascading.) The values S^*_λ/S_λ when a fraction I of the resonance radiation is imprisoned, is:

$$\frac{S^*_\lambda(I)}{S_\lambda} = \frac{S^*_\lambda(I=1)}{S_\lambda}\cdot I + \frac{S^*_\lambda(I=0)}{S_\lambda}(1 - I) \qquad (20)$$

$\frac{S^*_\lambda(I=1)}{S_\lambda}$ and $\frac{S^*_\lambda(I=0)}{S_\lambda}$ are found in Table IV

Degrees of imprisonment for some geometrics have been calculated by Phelps (1958)[12].

The S^*_λ/S_λ values in Table IV are uncertain partly due to the extrapolation procedures used to obtain cross sections, lifetimes and transition probabilities, partly due to the simplified model of the cascading used here. The error due to the extrapolation procedures (Appendix III.1.4 and III.2) is estimated from how well the extrapolations fit the quantities where they are well known. The error due to the model is discussed in Appendix III.1.3. The result is an uncertainty in the S^*_λ/S_λ of typically 50% of the difference from 1:

$$\Delta\left(\frac{S^*_\lambda}{S_\lambda}\right) \approx 0.5 \left|1 - \frac{S^*_\lambda}{S_\lambda}\right| \qquad (21)$$

The values of S^*_λ/S_λ in Table IV are therefore not accurate enough to be used to correct measured line intensities for the redistribution of cascading. They show, however, that some lines are little affected, as 5048Å, 4438Å, 4922Å and 4388Å at zero imprisonment, and 4713Å and 4121Å at all degrees of imprisonment.

The values in Table IV are calculated only for T_e = 10 eV. A complete calculation of S^*_λ/S_λ for many electron temperatures has not been done, but some samples show that the quantity $|1 - S^*_\lambda/S_\lambda|$ generally varies less than a factor of two from what Table IV gives, when T_e varies between 5 and 100 eV. With increasing T_e, the S^*_λ/S_λ values increase for triplet levels and decrease for singlet levels. This is mainly a result of the difference in energy dependence between the $1^1S\rightarrow$(triplet levels) and the $1^1S\rightarrow$(singlet levels) cross sections.

5. SUMMARY AND CONCLUSIONS REGARDING T_e-DETERMINATION FROM THE "SINGLET-TO-TRIPLET" INTENSITY RATIO.

The secondary processes examined in the three previous sections give limits to when the singlet-to-triplet line intensity ratio can be used for electron temperature determination. The influence of secondary processes on the line intensitites (S^*_λ/S_λ) compared to the T_e dependence of the line intensity ratios gives the following approximate error in the T_e-determination, if the line intensities are used with secondary processes disregarded:

S^*_λ/S_λ	Error factor in T_e (both multiplication and division)
$0.9 < S^*_\lambda/S_\lambda < 1.1$	< 1.2
$0.8 < S^*_\lambda/S_\lambda < 1.25$	< 1.5
$0.7 < S^*_\lambda/S_\lambda < 1.4$	< 2

The requirement corresponding to an error in T_e less than a factor of less than 1.5 is

$$0.8 < S^*_\lambda/S_\lambda < 1.25 \qquad (22)$$

This is evaluated below as limits to the experimental parameters. The result is summarized in Table V.

5.1. Influence on T_e-determination from excitation from metastables

Excitation from 2^1S and 2^3S in equilibrium population gives an influence on line intensitites that depends weakly on the electron temperature and the degree of imprisonment, but not on the electron or neutral He density. S^*_λ/S_λ values for eight He I lines are summarized in Tables II and III. For the triplet lines, they lie typically between 3 and 10. For the singlet lines, only upper limits on S^*_λ/S_λ can be given with some certainty. This upper limit varies between 2 and 20.

Since the cross sections involved are not known well enough, it is impossible to make corrections for this excitation process, and hence temperature determination by means of the line intensity ratio method becomes highly uncertain in all plasmas where the metastables have reached equilibrium population. However, in two situations the metastable level population can be below the equilibrium value: short-duration and low-density experiments.

5.1.1. Short-duration experiments

In an experiment with a time duration t_{ex}, much shorter than the time t_r for build-up of an equilibrium population, the S^*_λ/S_λ value is approximately (Section 2.3):

$$\frac{S^*_\lambda}{S_\lambda} \approx 1 + \frac{t_{ex}}{t_r} \left| \left(\frac{S^*_\lambda}{S_\lambda} \right)_{eq.met} - 1 \right| \qquad (23)$$

t_r is found in Table I and $(S^*_\lambda/S_\lambda)_{eq.met}$ in Tables II and III. The condition:

$$0.8 < S^*_\lambda/S_\lambda < 1.25 \qquad =(22)$$

inserted in (23) gives the limits on the product $n_e\ t_{ex}$ in column one of Table V.

5.1.2. Low-density experiments

In low-density experiments, t_r can be long compared to the time t_{diff} for diffusion of a metastable atom out of the laboratory plasma. When the mean free path is longer than a typical length L of the plasma, and the metastables have room temperature,

t_{diff} is:

$$t_{diff} \approx \frac{L}{V_{thermal}} \approx 10^{-3}\ L \qquad (24)$$

When $t_{diff} < t_r$, the S^*_λ/S_λ is (Section 2.3):

$$\frac{S^*_\lambda}{S_\lambda} \approx 1 + \frac{t_{diff}}{t_r}\left|\left(\frac{S_\lambda}{S_\lambda}\right)_{eq.met.} - 1\right| \qquad (25)$$

(24), (25), and the condition (22) on S^*_λ/S_λ gives the limits on the product n_e L in column two of Table V.

5.2. Influence on T_e-determination from excitation transfer collisions

Excitation transfer collisions give an influence on line intensitites that depends on electron temperature, electron density and degree I of imprisonment of resonance radiation. S^*_λ/S_λ values for eight He I lines, for 5 eV $\lesssim T_e \lesssim$ 100 eV, $10^{14} m^{-3} \lesssim n_e \lesssim 10^{19} m^{-3}$ and 0% $\lesssim$ I $\lesssim$ 100% are given in Fig. 3a-d. Typical values lie between 0.1 and 10 for lines with D levels for upper levels. T_e-determination from the line intensity ratio can be seriously influenced by excitation transfer in plasmas with $n_e > 10^{16} m^{-3}$.

The condition (22) on S_λ/S_λ for the excitation transfer process gives an upper limit for n_e that depends on T_e and I. Table V, columns three and four, gives the limit for some combinations of T_e and I.

5.3. Influence on T_e-determination from redistribution of cascading

The values of S^*_λ/S_λ for this process lie typically between 0.9 and 1.5 (Table IV). They depend on n_e and I, and to a lesser degree on the electron temperature. Most lines are little influenced by the redistribution of cascading, as 5048Å, 4438Å, 4922Å and 4388Å at zero degree of imprisonment and 4713Å and 4121Å at all degrees of imprisonment. For other lines, particularly lines with D levels for upper levels at high degrees of imprisonment, the intensities can be increased with factors up to 2. These lines should therefore be used with caution for T_e-determination.

6. T_e-DETERMINATION FROM ABSOLUTE LINE INTENSITY MEASUREMENTS

The previous sections have treated T_e-determination from relative line intensities. Alternatively, the electron temperature may be determined from the absolute intensities of single spectral lines. This method is experimentally more complicated than the method based on relative line intensitites, since it requires absolute calibration of the detecting system, and measurements of both the electron and neutral helium densities in the light-emitting region. On the other hand, it is more sensitive to the electron temperature and less sensitive to secondary processes: While the singlet-to-triplet line intensity ratios vary typically by a factor 5÷10 when T_e varies between 5 and 100 eV, the intensities of single lines vary by a factor of 100 or more. This strong T_e dependence also makes the absolute intensity method less sensitive to spatial variations in n_e.

The measured quantity is the signal L from the light detecting system:

$$L = C \int_V N_\lambda dV \qquad (26)$$

where the integral is taken over the volume V that emits light to the measuring system taking the appropriate acceptance solid angle of the spectrograph into account. C is a calibration constant. N_λ is the emission rate of the line $\left[\text{photons} \cdot m^{-3} \cdot s^{-1}\right]$, which can be expressed with the use of the apparent excitation rate coefficient S_λ^* :

$$N_\lambda = n_e \, n_{He(1^1S)} \, S_\lambda^* \qquad (27)=(1)$$

If S_λ^* is assumed to be constant in the volume V, (26) and (27) give S_λ^* as a function of measured quantities:

$$S_\lambda^* = \frac{L}{C \int_V n_e \, n_{He(1^1S)} \, dV} \qquad (28)$$

The electron temperature is obtained from S_λ^* on the assumption that no secondary processes influence the line intensity, so that $S_\lambda = S_\lambda^*$. S_λ can be taken from Fig. 5.

The assumption $S_\lambda = S_\lambda^*$ gives an error in T_e that depends on how sensitive the line is to secondary processes, and on how S_λ varies with T_e. The four lines 5016Å (3^1P-2^1S), 3889Å (3^3P-2^3S), 4922Å (4^1D-2^1P) and 4713Å(4^3S-2^3P) seem to be best suited among the He I lines for this kind of T_e-determination. For these four lines, the limits on the experimental parameters are calculated below, for which the secondary processes give an uncertainty in the T_e-determination of less than a factor 1.1, 1.2 or 1.5. The result is summarized in the Tables VI and VII a-d. Table VI gives typical values of the limiting parameters, and can be used to quickly establish whether a line is suitable or not for T_e-determination in a particular experimental situation. Table VII a-d gives more detailed information for each line.

6.1 Calculations

6.1.1. Sensitivity of lines to T_e-variations

S_λ as a function of T_e (Appendix I.1.1) gives how much S_λ^* can be allowed to differ from S_λ, when the uncertainty in the T_e-determination shall be less than a factor 1.1, 1.2 or 1.5 (both multiplication and division). This was calculated for the lines 5016Å, 3889Å, 4713Å and 4922Å, and for temperatures T_e = 5, 10, 20, 30, 40, 50, 100 and 200 eV.

6.1.2. Excitation from metastables

Excitations to the upper line levels from the metastable levels are treated as in Sections 2 and 5.1 above. Equations (8) and (10) together with the limits on S_λ^*/S_λ from 6.1.1. give the limits on the product $n_e t_{ex}$ in Tables VI and VII (t_{ex} = experimental time). In a low-density plasma, the limit on $n_e t_{ex}$ can be replaced by an upper limit on $n_e L$ as discussed in section 5.1.2:

$$(n_e L)_{limit} \approx 10^3 \, (n_e t_{ex})_{limit} \qquad (29)$$

where L = typical apparatus dimension.

6.1.3. Excitation transfer and imprisonment of resonance radiation

For the two lines 4922Å and 4713Å, the combined influence on S_λ^*/S_λ from these processes are calculated in Section 3. The influence on the 3889Å line is treated in the same way (solution of the

system of coupled rate equations (11)). The result of these calculations is combined with the limits on S^*_λ/S_λ from 6.1.1. to give the limits on I and n_e for 4922Å, 4713Å and 3889Å in Tables VI and VII.

For the 5016Å line (3^1P-2^1S), a somewhat different approach is more suitable, since the upper level 3^1P is optically connected to the ground state. The large 3^1P-1^1S transition probability makes the 3^1P population little influenced (always less than 5%) by excitation transfer. As a consequence, the 5016Å line can be used without restriction on the electron density.

On the other hand, the influence of imprisonment of resonance radiation is stronger than for the other lines. The S^*_λ/S_λ value as a function of I is calculated with the use of the apparent branching ratio B^* (see Appendix I.2) for the 3^1P-2^1S transition. With the transition probabilities taken from Gabriel and Heddle (1960) , we get:

$$\frac{S^*_{5016}}{S_{5016}} = 1 + 43\ I \qquad (30)$$

This, and the limits on S^*_λ/S_λ from 6.1.1 gives the limits on I for the 5016Å line (Tables VI and VIIa).

7. Summary

It is found that the possibility to determine plasma electron temperature from intensities of neutral He lines is seriously limited by secondary processes. Most dominating are excitation from the metastable 2^3S level and excitation transfer in electron-atom collisions combined with imprisonment of resonance radiation.

Due to these processes, T_e-determination from relative line intensitites is limited to low-density, short-duration plasmas (typically $n_e < 2\cdot10^{16}m^{-3}$, $t_{ex} < 5\cdot10^{-6}s$) or to even lower densities that depend on the apparatus dimensions (typically $n_e < 3\cdot10^{15}m^{-e}$, $L \approx 0.1$ m).

For T_e-determination from absolute line intensitites the situation is more favourable, and with a suitable choise of lines the restrictions on n_e and t_{ex} can be typically ($n_e < 5\cdot10^{17}m^{-3}$, $t_{ex} < 10^{-5}s$) or ($n_e < 10^{17}m^{-3}$, $L \approx 0.1$ m) for electron tempera-

tures above 10 eV. For temperatures below 10 eV and degrees of imprisonment below 7% measurements are possible for electron densities up to 10^{19} or $10^{20} m^{-3}$, and without any limits on t_{ex} or L.

Acknowledgements

The author is indebted to Prof.C.-G. Fälthammar and dr:s I. Axnäs, L. Lindberg and M. Raadu for valuable discussions during the course of this work, to mrs G. Bylund for help with calculations and to mrs K. Forsberg for making the drawings.

The projekt has been financed by the Swedish Atomic Research Council.

APPENDIX I

I.1 Cross sections used to solve Equation (8)

1.1.1. $S_{1^1S\to j}$

For excitations from the ground state, the cross sections measured by St John et al. (1964) are used together with measurements close to threshold by Smit et al. (1963). Rate coefficients in this and the following sections are calculated by integration of close analytical fits to the cross sections over Maxwellian electron distributions.

Line excitation rates S_λ are obtained by dividing $S_{1^1S\to j}$ with the branching ratio $B_{j\to k}$ for the transition corresponding to λ.

$$B_{j\to k} = \sum_{\substack{\text{all } \ell \text{ with} \\ n_e \leq n_j}} A_{j\to \ell} \,/A_{j\to k} \qquad \text{(I)}$$

Transition probabilities are taken from those compiled by Gabriel and Heddle .

Fig. 5 shows ten line excitation rates obtained in this way. Part of the cross sections for single-collision excitations from the ground state to j come from excitations to high-lying levels, followed by cascading to j. This process is included in $S_{1^1S\to j}$. In Section 4, we need cross sections and excitation rates $N_{1^1S\to j}$ where the cascading is excluded. These quantities are denoted $S'_{1^1S\to j}$ and $N'_{1^1S\to j}$.

I.1.2 $\Sigma^1S_{1^1S\to 2^1S}$

Excitation from the ground state to 2^1S goes mainly by three routes:

- Direct excitation $1^1S\to 2^1S$ in one collision
- Excitation $1^1S\to n^1P$, followed by cascading $n^1P\to 2^1S$. The cascading is influenced by the degree of imprisonment.
- Excitation $1^1S\to 2^3S$ (see I.1.3), followed by excitation transfer $2^3S\to 2^1S$ in an electronic collision.

The $1^1S \rightarrow 2^1S$ and $1^1S \rightarrow n^1P$ cross sections is obtained by extrapolition from the cross sections used in I.1.1. The cross sections to levels with the same orbital quantum number are assumed to have the same energy dependence and vary with the n quantum number as n^{-3}.

The $n^1P \rightarrow 2^1S$ cascading is calculated with the use of the transition probabilities compiled by Gabriel and Heddle, and the $2^3S \rightarrow 2^1S$ cross section is taken from Drawin (1966). The influence on the $n^1P \rightarrow 2^1S$ cascading from imprisonment is taken into account as described in I.2.

I.1.3 $\Sigma^1S_{1^1S \rightarrow 2^3S}$

All excitations from the ground state to triplet levels end up in 2^3S after cascading, with the dominating contribution (85%) coming from the levels with n = 2 and 3. A total cross section is obtained by adding all $1^1S \rightarrow$triplet levels cross sections (taken from I.1.1 or extrapolated as in I.1.2). An experimental determination of this total cross section close to maximum has been made by Bogdanova et al. (1975). Their results agree with our calculated value.

I.1.4 $\Sigma^2S_{2^1S \rightarrow 2,\ 1^1S}$

The dominating process at degrees of imprisonment $\lesssim$ 98% is excitation $2^1S \rightarrow 2^1P$, followed by an optical transition $2^1P \rightarrow 1^1S$. The sum is then given by:

$$\Sigma^2S_{2^1S \rightarrow i,\ 1^1S} = S_{2^1S \rightarrow 2^1P} \left[B^*_{2^1P \rightarrow 1^1S} \right]^{-1} \qquad \text{(II)}$$

where $B^*_{2^1P \rightarrow 1^1S}$ is the "apparent bramching ratio" for the transition with imprisonment taken into account as described in I.2. The $2^1S \rightarrow 2^1P$ excitation cross section has been calculated both with the Born approximation and with the Vainshtein, Presnyakov and Sobelman (VPS) approximation by Flannery et al. (1975). The difference between the two approximations is the reason for the uncertainty in Table I., where the relaxation time t_r for build-up of equilibrium population is calculated. t_r is determined by the de-exciting process:

$$t_r = \left[n_e \ \Sigma^2S_{2^1S \rightarrow 1^1S} \right]^{-1} \qquad \text{(III)}$$

with notations as in Section 2.1.

I.1.5 $\Sigma^2S_{2^1S\to i,\ 1^1S}$

Drawin (1966) has given the electron impact ionization cross section. This process dominates over $2^3S\to1^1S$ deexcitation, which is discussed by Nesbet et al. (1974).

I.1.6 $S_{2^1S\to i}$ and $S_{2^3S\to i}$

Theoretical cross sections for the $2^3S\to3^3S$, $2^3S\to3^3D$, $2^1S\to3^1S$ and $2^1S\to3^1D$ excitations by electron impact have been calculated by Flannery et al. (1975). They used both the Born and the VPS approximation and state that the difference between them (typically a factor of 3) can be taken as a measure of the uncertainty. Since we need cross sections for excitation to higher lying levels than Flannery et al:s calculations cover, these have been extrapolated in the following way. The shape of the cross section (as a function of the electron energy W_e) is assumed to be the same for levels with the same orbital quantum number. The relative magnitude is assumed to be 1, 1/3 and 1/6 for excitations to the levels with main quantum number n = 3, 4 and 5, respectively. These relative magnitudes are founded on the relative magnitudes of the $2^{1,3}S\to3^{1,3}P$ and $2^{1,3}\to4^{1,3}P$ cross sections calculated by Flannery et al. and the $2^{1,3}\to4^{1,3}P$ and $2^{1,3}\to5^{1,3}P$ cross sections given by Drawin[16].
The error in this extrapolation procedure is estimated to be less than the difference between the Born and VPS approximations.

I.2 Connection between I and cascading from n^1P levels

We define an "apparent branching ratio" B^* for the $n^1P\to1^1S$ transitions so that the fraction of the (non-radiative) excitations to the n^1P levels that give escaping resonance radiation is $(B^*_{n^1P\to1^1S})^{-1}$. This apparent branching ratio is then a function $B^*_{n^1P\to1^1S}(I)$ of I. The degree of imprisonment is given by the reduction in escaping radiation:

$$I = \frac{(B^*_{n^1P\to1^1S}(0))^{-1} - (B^*_{n^1P\to1^1S}(I))^{-1}}{(B^*_{n^1P-1^1S}(0))^{-1}} \qquad \text{(IV)}$$

where $B^*_{n^1P\to1^1S}(0)$ is the branching ratio for zero imprisonment, given by Equation I. I and IV give:

$$B^{*}_{n^1P\to 1^1S}(I) = \frac{\sum_{\text{all } \ell} A_{n^1P\to \ell}}{A_{n^1P\to 1^1S}(1-I)} \qquad \text{(V)}$$

which is used in Section I.1.4.

The apparent branching ratio for $n^1P\to 2^1S$ cascading used in I.1.2 is obtained from (V) and:

$$(B^{*}_{n^1P\to 1^1S}(I))^{-1} + (B^{*}_{n^1P\to 2^1S}(I))^{-1} = 1 \qquad \text{(VI)}$$

Here, cascading from n^1P levels to m^1S levels with $n \geq 3$ has been neglected. This gives an error $\leq 15\%$ in $B^{*}_{n^1P\to 2^1S}$.

APPENDIX II DATA USED TO SOLVE EQUATION (11)

II.1 Excitation transfer collisions

For the transitions indicated by arrows in Fig. 1, the Born-Bethe approximation is used, as given by Drawin (1966).

$$\sigma_{ij} = 4\pi \frac{E_1^H}{E_{ij}} |Z_{ij}|^2 \left(\frac{E_{ij}}{E_e}\right)^2 \left(\frac{E_e}{E_{ij}} - 1\right) \ln \left(1.5 \frac{E_e}{E_{ij}}\right) \qquad \text{(VII)}$$

where E_1^H is 13.59 eV, E_e is the electron energy, E_{ij} is the energy difference $|E_i - E_j|$ between the levels i och j, and Z_{ij} the dipole length for the transition i→j. The dipole lengths for these transitions in excited helium are very close to the corresponding dipole lengths for hydrogen, which are used instead. Values are given by Bethe and Salpeter (1957). The quantity $|Z_{ij}|^2$ (and therefore the cross section) is approximately proportional to n^4.

The cross section equation (VII) is used in Section 3 for optically allowed excitation transfers with a change in main quantum number. Equation (11) is only valid when such excitation transfers can be neglected.

II.2 Natural lifetimes

The natural lifetimes of many levels have been calculated by Thompson and Fowler (1975). For the remaining levels they are calculated from

$$\tau_i = \left(\sum_{\substack{\text{all } j \text{ with} \\ n_j \leq n_i}} A_{i \to j} \right)^{-1} \qquad \text{(VIII)}$$

with the use of the transition probabilities given by Wiese et al. (1966).

II.3 Apparent lifetimes of n^1P levels

From the apparent branching ratio $B^*_{i \to j}$(I), defined in I.2, an apparent transition probability $A^*_{n^1P-i^1S}$ is defined (in analogy with the definition of B, Equation I) by:

$$B^{*}_{n^1P\to 1^1S}(I) = \frac{A^{*}_{n^1P\to 1^1S}(I) - A_{n^1P\to 1^1S} + \sum_j A_{n^1P\to j}}{A^{*}_{n^1P\to 1^1S}(I)} \qquad \text{(IX)}$$

and an apparent lifetime $\tau^{*}_{n^1P}(I)$ in analogy with Equation VIII:

$$\tau^{*}_{n^1P}(I) = \frac{1}{A^{*}_{n^1P\to 1^1S}(I) - A_{n^1P\to 1^1S} + \sum_j A_{n^1P\to j}} \qquad \text{(X)}$$

(IV), (VIII), (IX) and (X) can be combined to give:

$$\tau^{*}_{n^1P} = \tau_{n^1P}\left(1 + I\frac{A_{n^1P\to 1^1S}}{\left[\sum_j A_{n^1P\to j}\right] - A_{n^1P\to 1^1S}}\right) \qquad \text{(XI)}$$

APPENDIX III

III.1 Determination of n_1 and n_2

The data needed to calculate n_1 and n_2 (Section 4.1) are:

III.1.1 Ionization cross section for high-lying levels

Cross sections for ionization by electron impact from excited H levels have been given by Percival (1966). For high-lying levels they should be applicable also for He:

$$\sigma(u_n) = \frac{(1.28\, n^{-1} \ell n\, (u_n\, n^{-2}) + 6.67)\,(u_n - 1)}{u_n^2 + 1.67\, u_n + 3.59}\, \pi\, a_o^2\, n^4 \qquad \text{(XII)}$$

$u_n = \frac{W_e}{W_{ni}}$ (W_{ni} = ionization energy from level n approximately $13.59\, n^{-2}$ [eV]).

III.1.2 Excitation transfer with a change in n

Ionization from a level can go via many excitation transfer collisions, each giving a small change in main quantum number. A change of n with $\pm$ 1 is more likely than changes greater than 1. Cross sections for these transitions for $n \leq 5$ have been calculated by Omidvar (1965) from the Born approximation cross section. For higher-lying states Saraph (1964) gives a formula, which agrees well with Omidvar's results at low n.

III.1.3 Excitation transfers without change in n

The Born approximation cross section (VII) is used with dipole lengths taken from Bethe and Salpeter[20] (see II.1).

III.1.4 Natural lifetimes

Lifetimes for high lying leves are obtained as follows:
For the levels with n = 3-7, measured lifetimes of n^1S levels are used, taken from Thompson and Fowler. The value at n = 7 is then taken as basis for an extrapolation with the lifetime proportional to $n^{4,5}$ (Bethe and Salpeter) for the average lifetime of the n:th quantum state. This extrapolation takes the longer lifetimes of levels with high azimuthal quantum number into account. For levels with

the same azimuthal quantum number, the lifetime varies as n^3, as used in Section 4.1.

III.1.4 Calculations

The data above are used to calculate the electron densities, at which on the average one collision of each type discussed above occurs during the natural lifetime of an excited atom. The results of the calculations are plotted in Fig. 4, electron density versus main quantum number. The curves, A, B and C correspond to the collisions discussed in III.1.1, III.1.2 and III.1.3, respectively.

The curves in Fig. 4 defining the limits n_1 and n_2 between group one, two and three in 4.1 are choosen in the following way:

On the curve marked n_1, there are on the average three excitation transfer collisions during a natural lifetime. This value is choosen by comparison with Section 3, where exact calculations are done for n = 4 and n = 5. Three collisions during a natural lifetime corresponds to a relative population approaching "horizonthal thermal equilibirum".

On the curve marked n_2, there is a 50% probability that an excitation will eventually lead to ionization rather than cascading.

It turns out that the S^*_λ/S_λ-values for the cascading are only little influenced if we change the number of collisions defining n_1 with a factor of two, or vary the probability defining n_2 between 25% and 75%. The uncertainties in S^*_λ/S_λ (Section 4.3) are based on this, and on estimated uncertainties in the cross sections and transition probabilities.

III.2 Data used to solve Equation (19)

The cross sections for excitation from the ground state to the high-lying states are extrapolated from the cross sections in Appendix I.1.1. They are assumed to vary as n^{-3} with the main quantum number, and the energy dependence of high n excitation cross sections are taken to be the same as that of the low n functions having the same azimuthal quantum number.

Transition probabilities for $n < 9$ have been compiled by Gabriel and Heddle. For the higher-lying levels (which only contribute marginally to the solution of Equation (16)) an extrapolation procedure is used.

References

Bethe, H.A. and Salpeter, E.E.: 1957, Quantum Mechanics of One and Two Electron Systems. Handbuch der Physik 35, p. 349.

Bogdanova, I.P. and Marusin, V.D.: 1975, Determination of the efficiency of electron-impact excitation of a metastable 2^3S Helium level. Opt. Spektrosk. 38, 189.

Brenning, N.: 1977, Electron Temperature Measurements in Low Density Plasmas by Helium Spectroscopy I. Royal Institute of Technology, report TRITA-EPP-77-24.

Cunningham, S.P.: 1955, Conference on Thermonuclear Reactions. U.S. Atomic Energy Commission Report No 279, p. 289.

de Vries, R.F. and Mewe, R.: 1966, Spectroscopic Determination of Electron Temperature in a Helium Plasma. Phys. Fluids 9, 414.

Drawin, H.W.: 1964, Besetzungsdichten angeregter He I-Atome in einem nicht-termischen Plasma. Z. Naturforsch. 19a, 1451.

Drawin, H.W.: 1966, Collision and Transport Cross Sections, EUR-CEA-FC-383 (Fontenay-aux-Roses).

Drawin, H.W.: 1966, Über die Temperaturbestimmung aus dem Intensitätsverhältnis I (Triplett)/I (Singnlett) zweier He I-Linien in nicht-thermischen Plasma. Z. Naturforsch. 22a, 587.

Eastlund, B.J., Spero, D., Johnson, M., Korn, P., Wharton, C.B., Wilson, E.R.: 1973, Optical Diagnostics of an ECRH Plasma. J. Appl. Phys. 44, 4930.

Flannery, M. R., Morrison, W.F., and Richmond, B.L.: 1975, Excitation in electron-metastable helium collisions. J. Appl. Phys. 46, 1186.

Gabriel, A.H. and Heddle, P.W.O.: 1960, Excitation processes in helium. Proc. R. Soc. A258, 124.

May, R.B. and Hughes, R.H.: 1967, Excitation Transfer in Helium. Phys. Rev. 154, 151.

Lin, C.C. and Fowler, R.G.: 1961, Theory of Collision Transfer of Excitation in Helium. Ann. Phys. 15, 461.

Lin, C.C. and StJohn, R.M.: 1962, Collisional Excitation Transfer to the 4^1D State in Helium by Multiple State Mechanism. Phys. Rev. 128, 1749.

Mewe, R.:1967, Note on the singlet and triplet population in Helium. Br. J. Appl. Phys. 17, 1239.

Nesbet, R.K., Oberoi, R.S. and Bardsley, J.N.: 1974, Deactivation of He 2^3S by Thermal Electrons. Chem. Phys. Lett. 25, 587.

Omidvar, K.: 1965, Excitation by Electron Collision of Excited Atomic Hydrogen. Phys. Rev. 140A, 38.

Percival, I.C.: 1966, Cross Sections for Collisions of Electrons with Hydrogen Atoms and Hydrogen-Like Ions.Nuclear Fusion 6, 182.

Phelps, A.V.: 1958, Effect of the Imprisonment of Resonance Radiation on Excitation Experiments. Phys. Rev. 110, 1362.

Saraph, H.F.: 1964, Cross Sections for n→n+1 transitions in hydrogen produced by electron impact. Proc. Phys. Soc. (London) 83, 763.

Smit, C., Heideman, H.G.M., and Smit, J.A.: 1963, Relative Optical Excitation Functions of Helium (Excitation by Electrons). Physica 29, 245.

Sovie, R.J.: 1964, Spectroscopic Determination of Electron Temperature and Percentage Ionization in a Helium Plasma. Phys. Fluids 7, 613.

StJohn, R.M., Miller, F.L., and Lin, C.C.: 1964, Absolute Electron Excitation Cross Sections of Helium. Phys. Rev. 134, 888.

Thompson, R.T. and Fowler, R.G.: 1975, Observations on Lifetimes and Excitation Processes for the Upper States in Atomic Helium. J. Quant. Spec. Rad. Transf. 15, 1017.

Wiese, W.L., Smit, M.W., and Glennon, B.M.: 1966, Atomic Transition Probabilities. (NSRDS-NB S4).

·el	Imprison-ment I ↓ \ T_e [eV] → (1 eV = 7740 K)	5	10	20	50	100	200
³S	$0 \leq I \leq 1$	$2.9 \cdot 10^{13}$	$1.2 \cdot 10^{13}$	$9.1 \cdot 10^{12}$	$7.1 \cdot 10^{12}$	$7.1 \cdot 10^{12}$	$7.7 \cdot 10^{12}$
	$0 < I \leq 0.5$	$3 \cdot 10^{11}$	$1.8 \cdot 10^{11}$	$1.7 \cdot 10^{11}$	$1.9 \cdot 10^{11}$	$2.2 \cdot 10^{11}$	$3.1 \cdot 10^{11}$
	$0.5 < I \leq 0.75$	$7.5 \cdot 10^{11}$	$4.5 \cdot 10^{11}$	$4.3 \cdot 10^{11}$	$4.8 \cdot 10^{11}$	$5.5 \cdot 10^{11}$	$7.8 \cdot 10^{11}$
	$0.75 < I \leq 0.85$	$1.5 \cdot 10^{12}$	$9 \cdot 10^{11}$	$8.5 \cdot 10^{11}$	$9.5 \cdot 10^{11}$	$1.1 \cdot 10^{12}$	$1.5 \cdot 10^{12}$
¹S	$0.85 < I \leq 0.90$	$2.5 \cdot 10^{12}$	$1.5 \cdot 10^{12}$	$1.4 \cdot 10^{12}$	$1.6 \cdot 10^{12}$	$1.8 \cdot 10^{12}$	$2.6 \cdot 10^{12}$
	$0.90 < I \leq 0.95$	$4.3 \cdot 10^{12}$	$2.6 \cdot 10^{12}$	$2.4 \cdot 10^{12}$	$2.7 \cdot 10^{12}$	$3.1 \cdot 10^{12}$	$4.4 \cdot 10^{12}$
	$0.95 < I \leq 0.98$	$8.6 \cdot 10^{12}$	$5.1 \cdot 10^{12}$	$4.9 \cdot 10^{12}$	$5.4 \cdot 10^{12}$	$6.3 \cdot 10^{12}$	$7.7 \cdot 10^{12}$
	$0.98 < I \leq 0.99$	$2 \cdot 10^{13}$	$1.2 \cdot 10^{13}$	$9.1 \cdot 10^{12}$	$7.1 \cdot 10^{12}$	$6.3 \cdot 10^{12}$	$7.7 \cdot 10^{12}$
	$0.99 < I \leq 1$	$2.9 \cdot 10^{13}$	$1.2 \cdot 10^{13}$	$9.1 \cdot 10^{12}$	$7.1 \cdot 10^{12}$	$6.3 \cdot 10^{12}$	$7.7 \cdot 10^{12}$

Table I Reduced relaxation time $n_e t_r$ [$m^{-3} s$] for build-up of equilibrium population of metastables. The values are uncertain within a factor of 2 (Section 2, Appendix I).

Line \ Imprisonment I	0%	10%	30%	50%
5048Å (4^1S-2^1P)	1.01 - 1.02	1.02 - 1.08	1.05 - 1.15	1.07 - 1.20
4438Å (5^1S-2^1P)	1.01 - 1.05	1.3 - 1.10	1.07 - 1.20	1.10 - 1.30
4922Å (4^1D-2^1P)	1.05 - 1.15	1.09 - 1.25	1.20 - 1.50	1.25 - 1.70
4388Å (5^1D-2^1P)	1.05 - 1.15	1.09 - 1.25	1.20 - 1.50	1.52 - 1.70

Table IIa S^*_λ/S_λ for excitations of some singlet lines from 2^1S in equilibrium population. T_e is between 5 and 200 eV (Section 2).

Line \ Electron temperature [eV] (1 eV= 7740 K)	5	10	20	50	100	200
5048Å (4^1S-2^1P)	< 19	< 9.0	< 5.0	< 3.1	< 2.0	< 1.5
4438Å (5^1S-2^1P)	< 18	< 8.4	< 6.4	< 4.4	< 2.6	< 1.7
4922Å (4^1D-2^1P)	< 52	< 19	< 11.5	< 6.9	< 4.4	< 3.0
4388Å (5^1D-2^1P)	< 37	< 16	< 11	< 8	< 5.7	< 4.6
5016Å (3^1P-2^1S) (only 0% imprisonment)	< 3.6	< 2.3	< 2.0	< 1.6	< 1.3	< 1.2

Table IIb S^*_λ/S_λ for excitations of some singlet lines from both 2^1S and 2^3S in equilibrium population, when $0 < I < 50\%$. Only upper limits can be obtained due to unknown cross sections for excitations from 2^3S (Section 2).

Line \ Electron temperature eV (1 eV= = 7740 K)	.5	.10	20	50	100	200
4713Å (4^3S-2^3P)	3.4 - 12	2.6 - 6.1	2.3 - 4.6	2.0 - 4.2	2.0 - 3.4	1.8 - 2.5
4121Å (5^3S-2^3P)	4.3 - 18	3.2 - 8.1	2.8 - 6.1	2.5 - 5.5	2.4 - 4.3	2.0 - 3.1
4472Å (4^3D-2^3P)	13 - 52	9.5 - 25	8.8 - 21	7.4 - 17	6.1 - 14	5.2 - 11
4026Å (5^3D-2^3P)	13 - 51	9.2 - 25	8.6 - 20	7.2 - 17	5.9 - 13	5.2 - 11
3889Å (3^3P-2^3S)	1.6 - 3.4	1.7 - 3.6	2 - 4	2 - 4	2 - 4	2 - 4

Table III S^*_λ/S_λ for excitations of some triplet lines from 2^1S and 2^3S in equilibrium population. Independent of degree of imprisonment (Section 2).

	Zero imprisonment				Complete imprisonment			
Level \ Electron density (m^{-3})	10^{14}	10^{15}	10^{16}	10^{17}	10^{14}	10^{15}	10^{16}	10^{17}
5048Å (4^1S-2^1P)	1.00	1.00	0.99	0.98	1.50	1.45	1.33	1.05
4438Å (5^1S-2^1P)	1.00	1.00	0.99	0.99	1.40	1.28	1.11	1.00
4922Å (4^1D-2^1P)	1.03	1.06	1.09	1.19	1.40	1.40	1.40	1.40
4388Å (5^1D-2^1P)	1.02	1.03	1.06	1.08	1.28	1.25	1.23	1.18
4713Å (4^3S-2^3P)	0.94	0.93	0.89	0.88	0.96	0.93	0.89	0.88
4121Å (5^3S-2^3P)	0.94	0.93	0.89	0.88	0.96	0.93	0.89	0.88
4472Å (4^3D-2^3P)	1.05	1.14	1.26	1.49	1.12	1.29	1.49	2.09
4026Å (5^3D-2^3P)	1.04	1.10	1.16	1.16	1.08	1.20	1.40	1.50

Table IV Values of S^*_λ/S_λ for the redistribution of the cascading contribution at electron densities between 10^{14} and 10^{17} m^{-3}, and an electron temperature of 10 eV. The uncertainty is typically 50% of the difference from 1 (Section 4).

	Due to excitations from metastable levels. One of the conditions shall be fulfilled.		Due to excitation transfer of atoms in upper line levels.		Due to redistribution of cascading. Both conditions shall be fulfilled.	
A ition)	Low density: Limit on product n_eL (L = typical length)	Short duration: Limit on product $n_e t_{ex}$ $[m^{-3}s]$	5eV < T_e < 30eV zero imprisonment	5eV < T_e < 30eV 100% imprisonment	Limit on n_e $[m^{-3}]$	Limit on degree of imprisonment
8A 2^1P)	$n_eL < 3\cdot10^{14}$	$n_e t < 3\cdot10^{11}$	$n_e < 2\cdot10^{16}$	$n_e < 10^{16}$	none	I < 30%
8A 2^1P)	$n_eL < 3\cdot10^{14}$	$n_e t < 3\cdot10^{11}$	$n_e < 2\cdot10^{15}$	$n_e < 5\cdot10^{15}$	none	I < 30%
2A 2^1P)	$n_eL < 10^{14}$	$n_e t < 10^{11}$	$n_e < 10^{18}$	$n_e < 5\cdot10^{15}$	none	I < 50%
8A 2^1P)	$n_eL < 10^{14}$	$n_e t < 10^{11}$	$n_e < 3\cdot10^{17}$	$n_e < 10^{15}$	none	I < 50%
3A 2^3P)	$n_eL < 5\cdot10^{14}$	$n_e t < 5\cdot10^{11}$	$n_e < 2\cdot10^{16}$	$n_e < 2\cdot10^{16}$	none	none
1A 2^3P)	$n_eL < 3\cdot10^{14}$	$n_e t < 3\cdot10^{11}$	$n_e < 10^{16}$	$n_e < 10^{16}$	none	none
2A 2^3P)	$n_eL < 10^{14}$	$n_e t < 10^{11}$	$n_e < 10^{16}$	$n_e < 10^{16}$	$n_e < 10^{15}$	none
5A 2^3P)	$n_eL < 10^{14}$	$n_e t < 10^{11}$	$n_e < 2\cdot10^{15}$	$n_e < 2\cdot10^{15}$	none	I < 40%

Table V Limits on experimental parameters from the condition that line intensities shall be influenced less than a factor 1.2 by secondary processes. This corresponds to an uncertainty in T_e-determination from the singlet-to-triplet intensity ratio with a factor 1.5 (both multiplication and division) (Section 5).

	Electron temperature T_e [eV]	Imprisonment of resonance radiation I [%]	Products $n_e t_{ex}$ [$m^{-3}s$] and $n_e L$ [m^{-2}]	Electron density n_e [m^{-3}]
5016Å (3^1P-2^1S)	$T_e < 10$ eV	I < 7%	No limit	No limit
	$10 < T_e < 100$	I < 0.5%	$n_e t_{ex} < 5 \cdot 10^{12}$ or $n_e L < 5 \cdot 10^{15}$	No limit
4922Å (4^1D-2^1P)	$T_e < 10$ eV	I < 50%	$n_e t_{ex} < 1.3 \cdot 10^{12}$ or $n_e L < 1.3 \cdot 10^{15}$	$n_e < 10^{18}$
	$10 < T_e < 50$	I < 20%	$n_e t_{ex} < 5 \cdot 10^{11}$ or $n_e L < 5 \cdot 10^{14}$	$n_e < 3 \cdot 10^{16}$
3889Å (3^3P-2^3S)	$T_e < 10$ eV	No limit	$n_e t_{ex} < 7.2 \cdot 10^{12}$ or $n_e L < 7.2 \cdot 10^{15}$	$n_e < 1.2 \cdot 10^{18}$
	$10 < T_e < 30$	No limit	$n_e t_{ex} < 1.2 \cdot 10^{12}$ or $n_e L < 1.2 \cdot 10^{15}$	$n_e < 3 \cdot 10^{17}$
4713Å (3^2S-2^3P)	$T_e < 10$ eV	No limit	$n_e t_{ex} < 5 \cdot 10^{12}$ or $n_e L < 5 \cdot 10^{15}$	$n_e < 10^{18}$
	10 eV $< T_e < 25$	No limit	$n_e t_{ex} < 5 \cdot 10^{11}$ or $n_e L < 5 \cdot 10^{14}$	$n_e < 10^{17}$

Table VI T_e-determination from absolute line intensities. Typical limits on experimental parameters, when the uncertainty in T_e is required to be less than a factor 1.5 (both multiplication and division) due to the influence of secondary processes on line intensities (Section 6). (The limit on $n_e L$ is only valid when the mean free path for He atoms is larger than L, and when the neutral He atoms have room temperature.)

5016Å (3^1P-2^1S)

Limited parameter →	I [%]			$n_e\ t_{ex}$ [$m^{-3}s$]		
Limiting process →	Excitation of 3^1P through absorption of resonance radiation			Excitation from 2^1S		
Accepted uncertainty factor in T_e →	1.1	1.2	1.5	1.1	1.2	1.5
T_e < 5 eV	< 2.3%	< 4.7%	< 21%	$< 1.2\cdot10^{13}$	$< 2.3\cdot10^{13}$	No limit
T_e = 10 eV	< 0.93%	< 2.3%	< 7.0%	$< 3.7\cdot10^{12}$	$< 9.6\cdot10^{12}$	No limit
T_e = 20 eV	< 0.70%	< 1.6%	< 2.8%	$< 2.7\cdot10^{12}$	$< 6.4\cdot10^{12}$	No limit
T_e = 50 eV	< 0.35%	< 0.70%	< 1.0%	$< 1.8\cdot10^{12}$	$< 3.6\cdot10^{12}$	$< 5.3\cdot10^{12}$
T_e = 100 eV	< 0.16%	< 0.28%	< 0.47%	$< 1.6\cdot10^{12}$	$< 2.8\cdot10^{12}$	$< 4.7\cdot10^{12}$

Table VIIa See text under Table VIId.

4922Å (4^1D-2^1P)

Limited parameter →	I [%]	n_e [m^{-3}]			$n_e\ t_{ex}$ [$m^{-3}s$]		
Limiting process →		Excitation transfer, combined with imprisonment of resonance radiation			Excitation from 2^1S		
Acceptabel uncertainty factor in T_e →		1.1	1.2	1.5	1.1	1.2	1.5
T_e < 5 eV	I = 0% I = 10% I = 100%	$< 10^{18}$ $< 10^{18}$ $< 2\cdot10^{16}$	$< 10^{18}$ $< 10^{18}$ $< 10^{17}$	$< 10^{18}$ $< 10^{18}$ $< 10^{18}$	$< 6\cdot10^{11}$	$< 1.1\cdot10^{12}$	$< 5.2\cdot10^{12}$
T_e = 10 eV	I = 0% I = 10% I = 100%	$< 10^{18}$ $< 10^{17}$ $< 10^{16}$	$< 10^{18}$ $< 10^{18}$ $< 2\cdot10^{16}$	$< 10^{18}$ $< 10^{18}$ $< 10^{18}$	$< 2.6\cdot10^{11}$	$< 6.7\cdot10^{11}$	$< 1.3\cdot10^{12}$
T_e = 20 eV	I = 0% I = 10% I = 100%	$< 10^{18}$ $< 5\cdot10^{16}$ $< 5\cdot10^{15}$	$< 10^{18}$ $< 10^{17}$ $< 10^{16}$	$< 10^{18}$ $< 2\cdot10^{17}$ $< 2\cdot10^{16}$	$< 1.5\cdot10^{11}$	$< 4.4\cdot10^{11}$	$< 6.9\cdot10^{11}$
T_e = 30 eV	I = 0% I = 10% I = 100%	$< 5\cdot10^{18}$ $< 3\cdot10^{16}$ $< 3\cdot10^{15}$	$< 10^{18}$ $< 5\cdot10^{16}$ $< 5\cdot10^{15}$	$< 10^{18}$ $< 10^{17}$ $< 10^{16}$	$< 1.1\cdot10^{11}$	$< 3.0\cdot10^{11}$	$< 4.5\cdot10^{11}$
T_e = 50 eV	I = 0% I = 10% I = 100%	$< 3\cdot10^{17}$ $< 2\cdot10^{16}$ $< 2\cdot10^{15}$	$< 10^{18}$ $< 2\cdot10^{16}$ $< 3\cdot10^{15}$	$< 10^{18}$ $< 3\cdot10^{16}$ $< 5\cdot10^{15}$	$< 7.1\cdot10^{11}$	$< 1.2\cdot10^{11}$	$< 1.8\cdot10^{11}$

Table VIIb See text under Table VIId

4713Å (4^1S-2^3P)

Limited parameter →	n_e [m^{-3}]			$n_e\ t_{ex}$ [$m^{-3}s$]		
Limiting process →	Excitation transfer			Excitation from 2 S		
Accepted uncertainty factor in T_e →	1.1	1.2	1.5	1.1	1.2	1.5
≤ 5 eV	$< 2\cdot10^{17}$	$< 10^{18}$	$< 10^{18}$	$< 2.6\cdot10^{12}$	$< 5.2\cdot10^{12}$	$< 2.4\cdot10^{13}$
10 eV	$< 10^{17}$	$< 2\cdot10^{17}$	$< 10^{18}$	$< 9.4\cdot10^{11}$	$< 2.4\cdot10^{12}$	$< 4.8\cdot10^{12}$
20 eV	$< 2\cdot10^{16}$	$< 10^{17}$	$< 2\cdot10^{17}$	$< 2.5\cdot10^{11}$	$< 5.1\cdot10^{11}$	$< 9.1\cdot10^{11}$
30 eV	$< 2\cdot10^{15}$	$< 2\cdot10^{16}$	$< 10^{17}$	$< 6.4\cdot10^{10}$	$< 1.0\cdot10^{11}$	$< 1.0\cdot10^{11}$

Table VIIc See text under Table VIId.

3889Å (3^3P-2^3S)

Limited parameter →	n_e [m^{-3}]			$n_e\ t_{ex}$ [$m^{-3}s$]		
Limiting process →	Excitation transfer			Excitation from 2^3S		
Accepted uncertainty factor in T_e →	1.1	1.2	1.5	1.1	1.2	1.5
$T_e \leq 5$ eV	$< 2.8\cdot10^{17}$	$< 9.7\cdot10^{17}$	$< 3.8\cdot10^{18}$	$< 1.2\cdot10^{13}$	$< 2.4\cdot10^{13}$	No limit
$T_e = 10$ eV	$< 2.2\cdot10^{17}$	$< 5.2\cdot10^{17}$	$< 1.2\cdot10^{18}$	$< 1.4\cdot10^{12}$	$< 4.2\cdot10^{12}$	$< 7.2\cdot10^{12}$
$T_e = 20$ eV	$< 7.1\cdot10^{16}$	$< 2.1\cdot10^{17}$	$< 9.6\cdot10^{17}$	$< 9.1\cdot10^{11}$	$< 2.3\cdot10^{12}$	$< 4.1\cdot10^{12}$
$T_e = 30$ eV	$< 4.8\cdot10^{16}$	$< 1.3\cdot10^{17}$	$< 3.2\cdot10^{17}$	$< 4\cdot10^{11}$	$< 8\cdot10^{11}$	$< 1.2\cdot10^{12}$

Table VIId Tables VII a-d show limits to when T_e-determination from absolute intensities of the He I lines 5016Å, 4922Å, 4713Å and 3889Å can be used. The limits are given for accepted uncertainty in the T_e-determination with factors 1.1, 1.2 and 1.5 (1 eV=7740 K). The limit on the product $n_e\ t_{ex}$ (t_{ex}= experimental time) can in a low-density plasma be replaced by a limit on the product n_e L, where L is a typical apparatus dimension. When the neutral helium is at room temperature and has a mean free path > L, the limits on n_e L can be calculated from the values above: $(n_e\ L)_{LIMIT} \approx 10^3\ (n_e\ t_{ex})_{limit}$ (Section 6).

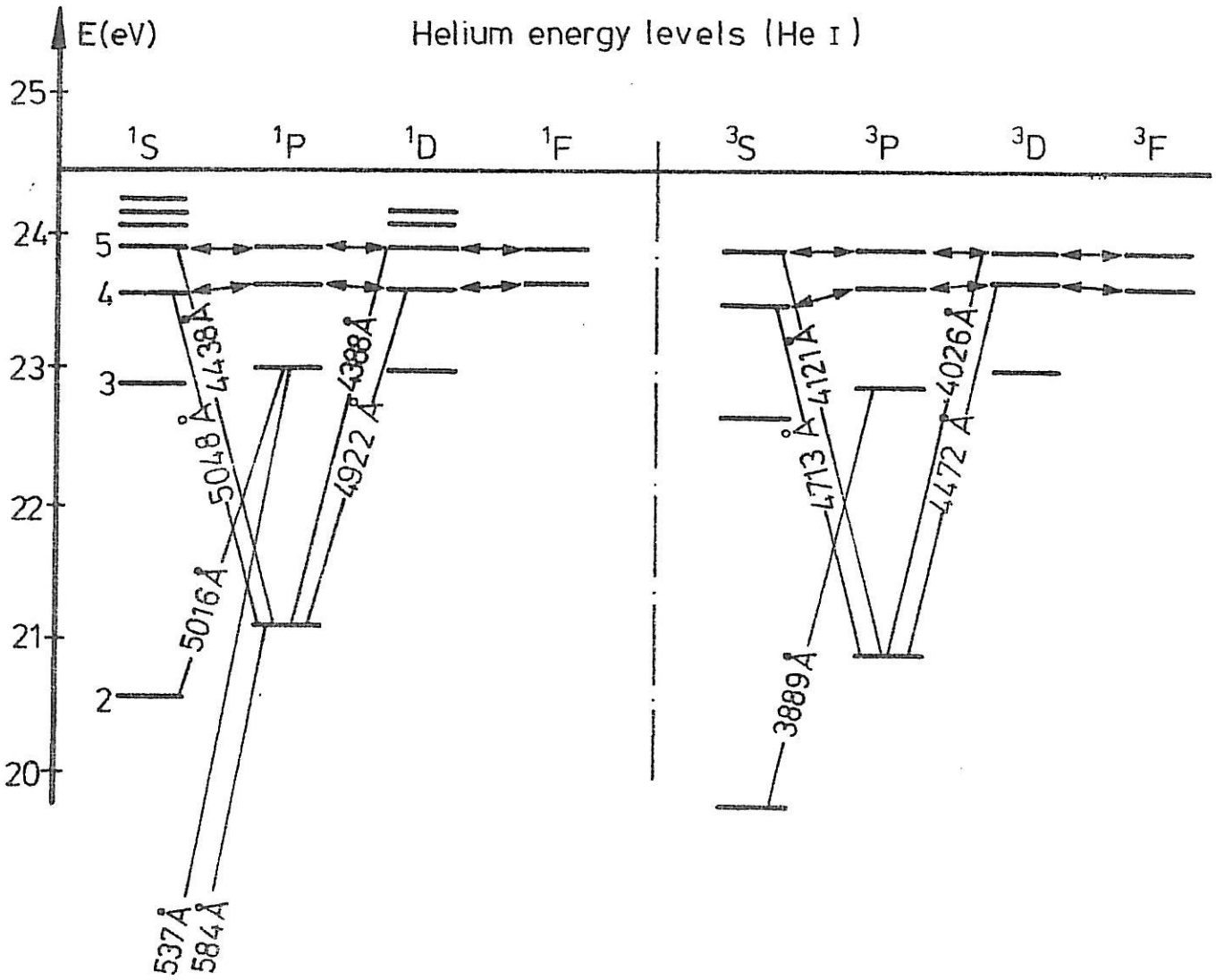

Fig. 1. Energy level diagram for neutral helium. The arrows indicate excitation transfer with large electron impact cross sections (Section 3).

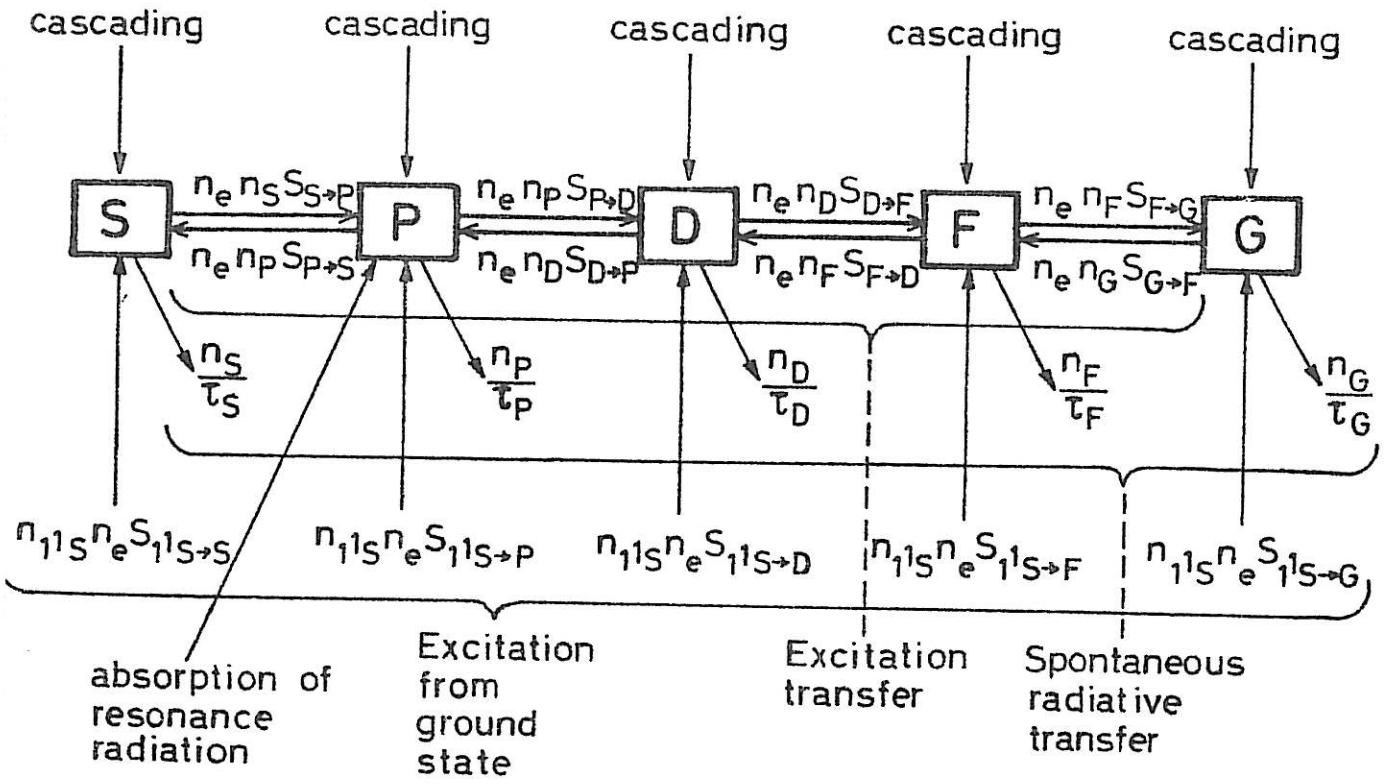

Fig. 2. The processes that populate and depopulate the levels in a group with the same main and spin quantum number. For collisional processes and radiative de-excitation the transition rates $[m^{-3}s^{-1}]$ are written at the arrows. S, P, D, F and G denote azimuthal quantum numbers (Section 3).

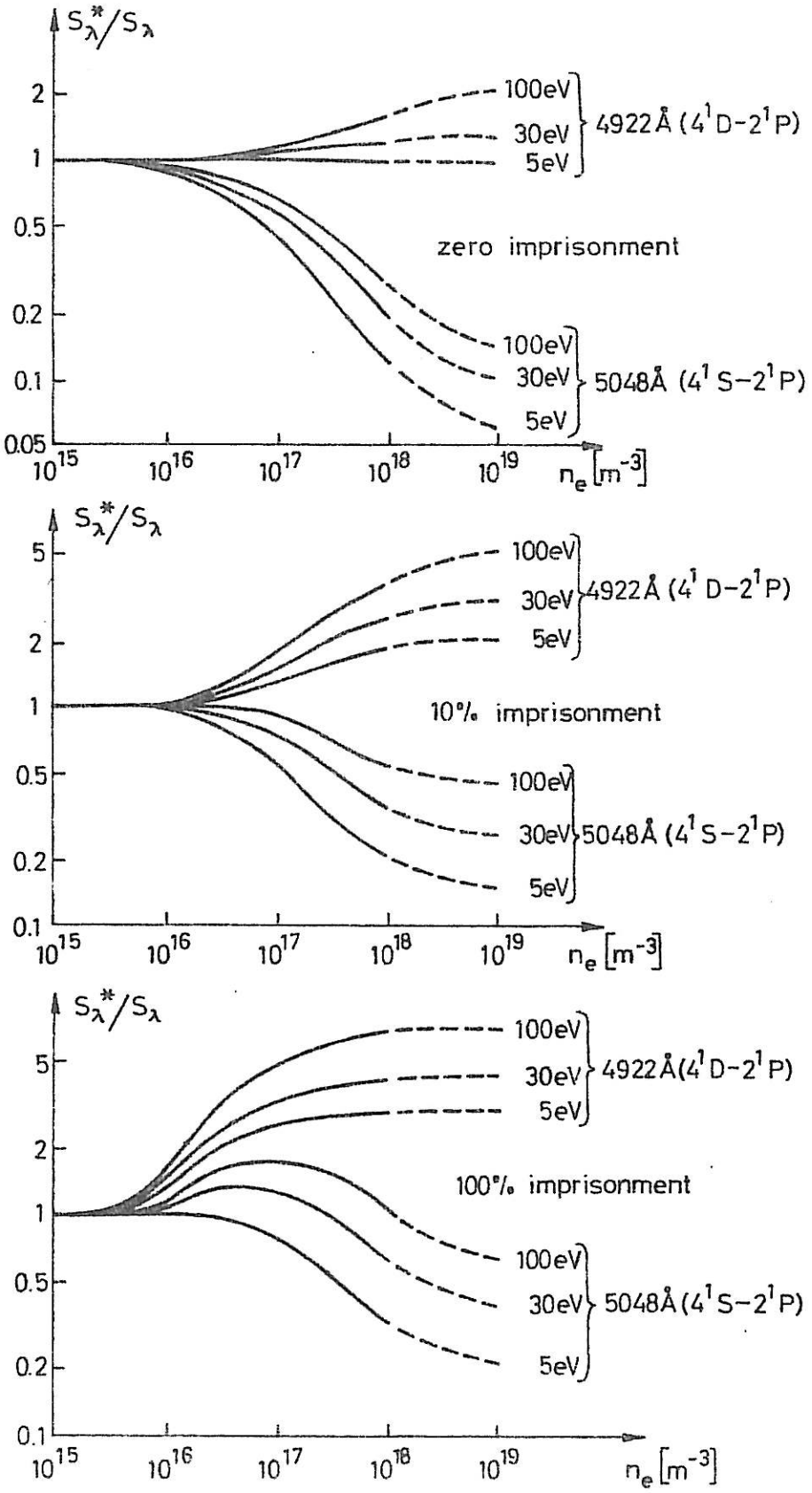
S_λ^*/S_λ
2
1
0.5
0.2
0.1
0.05
100eV
30eV
5eV
4922Å (4^1D-2^1P)
zero imprisonment
100eV
30eV
5eV
5048Å (4^1S-2^1P)
10^{15} 10^{16} 10^{17} 10^{18} 10^{19} n_e [m^{-3}]
S_λ^*/S_λ
5
2
1
0.5
0.2
0.1
100eV
30eV
5eV
4922Å (4^1D-2^1P)
10% imprisonment
100eV
30eV
5eV
5048Å (4^1S-2^1P)
10^{15} 10^{16} 10^{17} 10^{18} 10^{19} n_e [m^{-3}]
S_λ^*/S_λ
5
2
1
0.5
0.2
0.1
100eV
30eV
5eV
4922Å(4^1D-2^1P)
100% imprisonment
100eV
30eV
5eV
5048Å(4^1S-2^1P)
10^{15} 10^{16} 10^{17} 10^{18} 10^{19} n_e [m^{-3}]

Fig. 3a

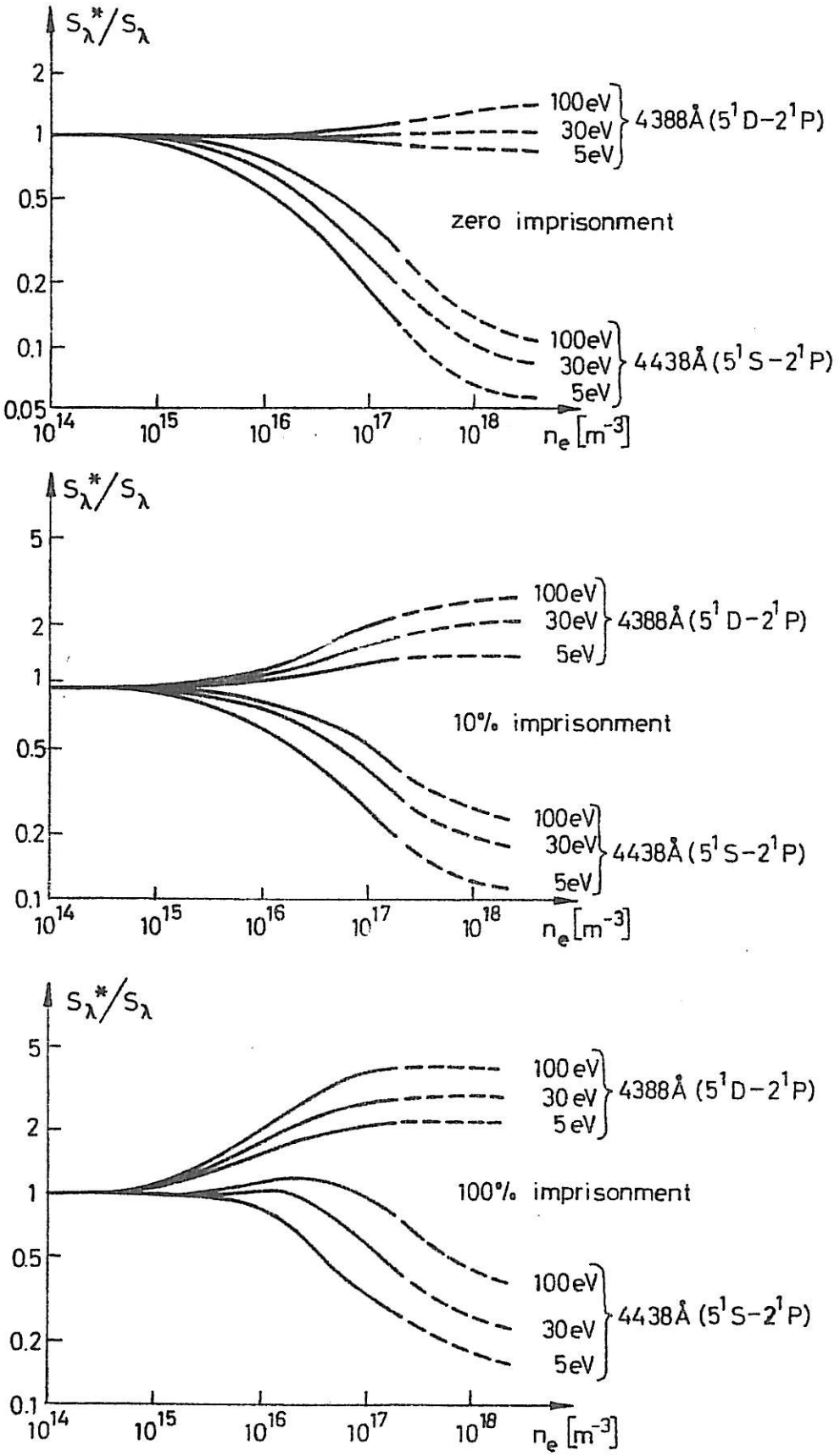
S_λ^*/S_λ
2
1
0.5
0.2
0.1
0.05
100eV
30eV
5eV
4388Å (5^1D-2^1P)
zero imprisonment
100eV
30eV
5eV
4438Å (5^1S-2^1P)
10^{14}
10^{15}
10^{16}
10^{17}
10^{18}
n_e [m^{-3}]
S_λ^*/S_λ
5
2
1
0.5
0.2
0.1
100eV
30eV
5eV
4388Å (5^1D-2^1P)
10% imprisonment
100eV
30eV
5eV
4438Å (5^1S-2^1P)
10^{14}
10^{15}
10^{16}
10^{17}
10^{18}
n_e [m^{-3}]
S_λ^*/S_λ
5
2
1
0.5
0.2
0.1
100 eV
30 eV
5 eV
4388Å (5^1D-2^1P)
100% imprisonment
100eV
30eV
5eV
4438Å (5^1S-2^1P)
10^{14}
10^{15}
10^{16}
10^{17}
10^{18}
n_e [m^{-3}]

Fig. 3b

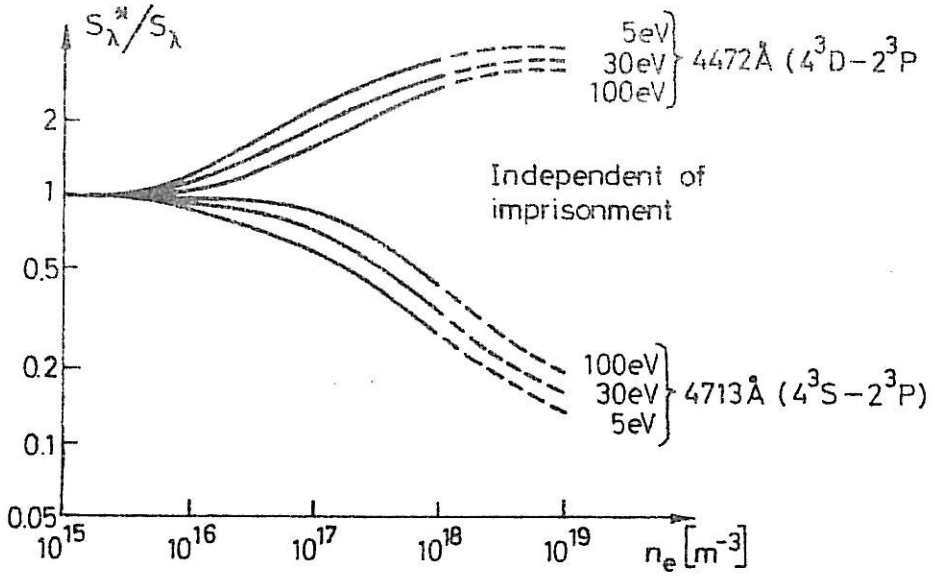

Fig. 3c

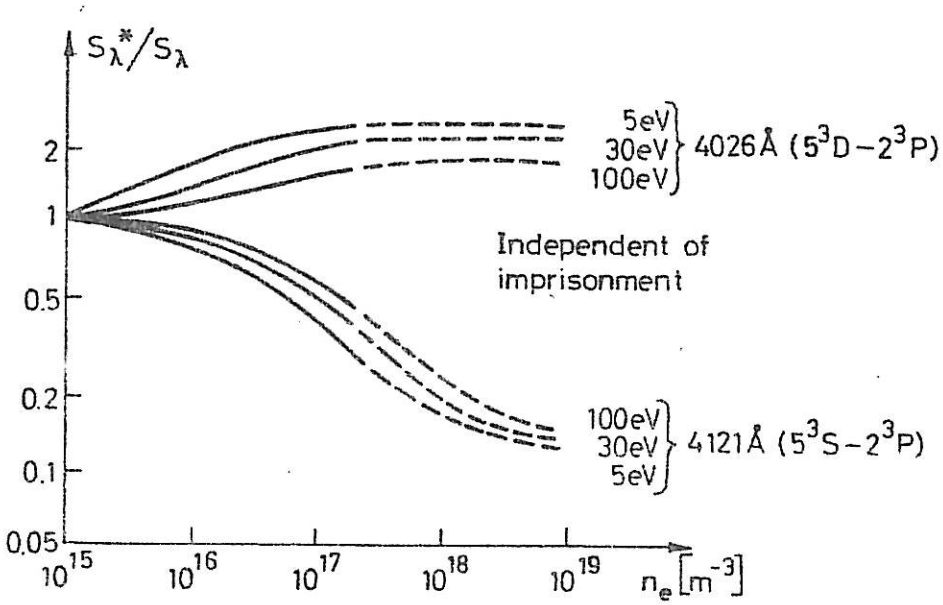

Fig. 3d

Fig. 3 a-d. Values of S_λ^*/S_λ for the excitation transfer process, for eight spectral lines, electron densities $10^{15} m^{-3} \leq n_e \leq 10^{19} m^{-3}$, degrees of imprisonment $0\% \leq I \leq 100\%$ and electron temperatures 5 eV $\leq T_e \leq$ 100 eV [1 eV = 7740 K]. The results are uncertain where the curves are dotted (Section 3).

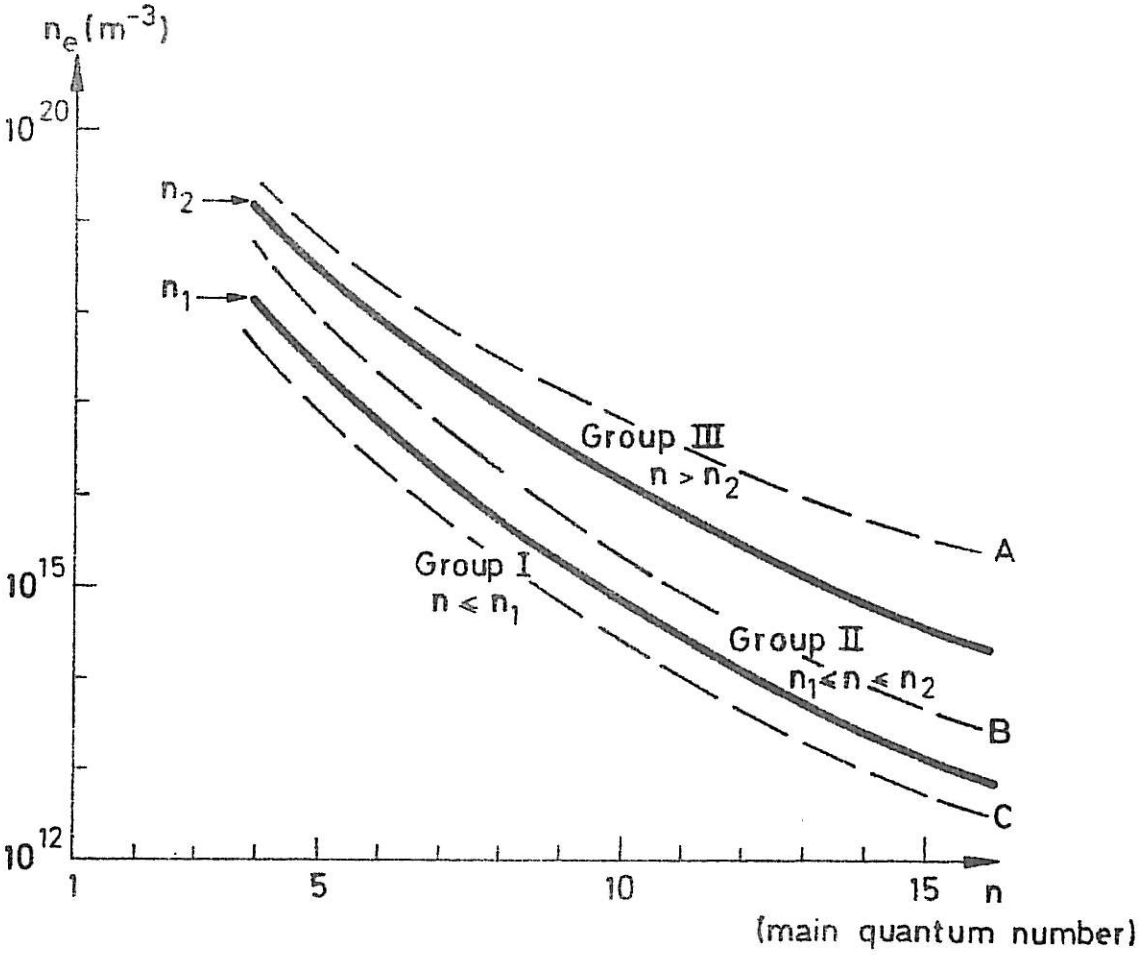

Fig. 4. Curves A, B and C gives combinations of n_e and n for which there is 50% probability of a particular kind of collision during the natural lifetime of a level. Curve A: ionization in one collision. Curve B: excitation transfer involving a change in n. Curve C: excitation transfer between levels with the same n. Curves n_1 and n_2 divide the levels in group one, two and three as described in Section 4 and Appendix III.1. The curves are calculated for T_e = 10 eV but are valid within a factor of two (in n_e) for 5 eV < T_e < 100 eV.

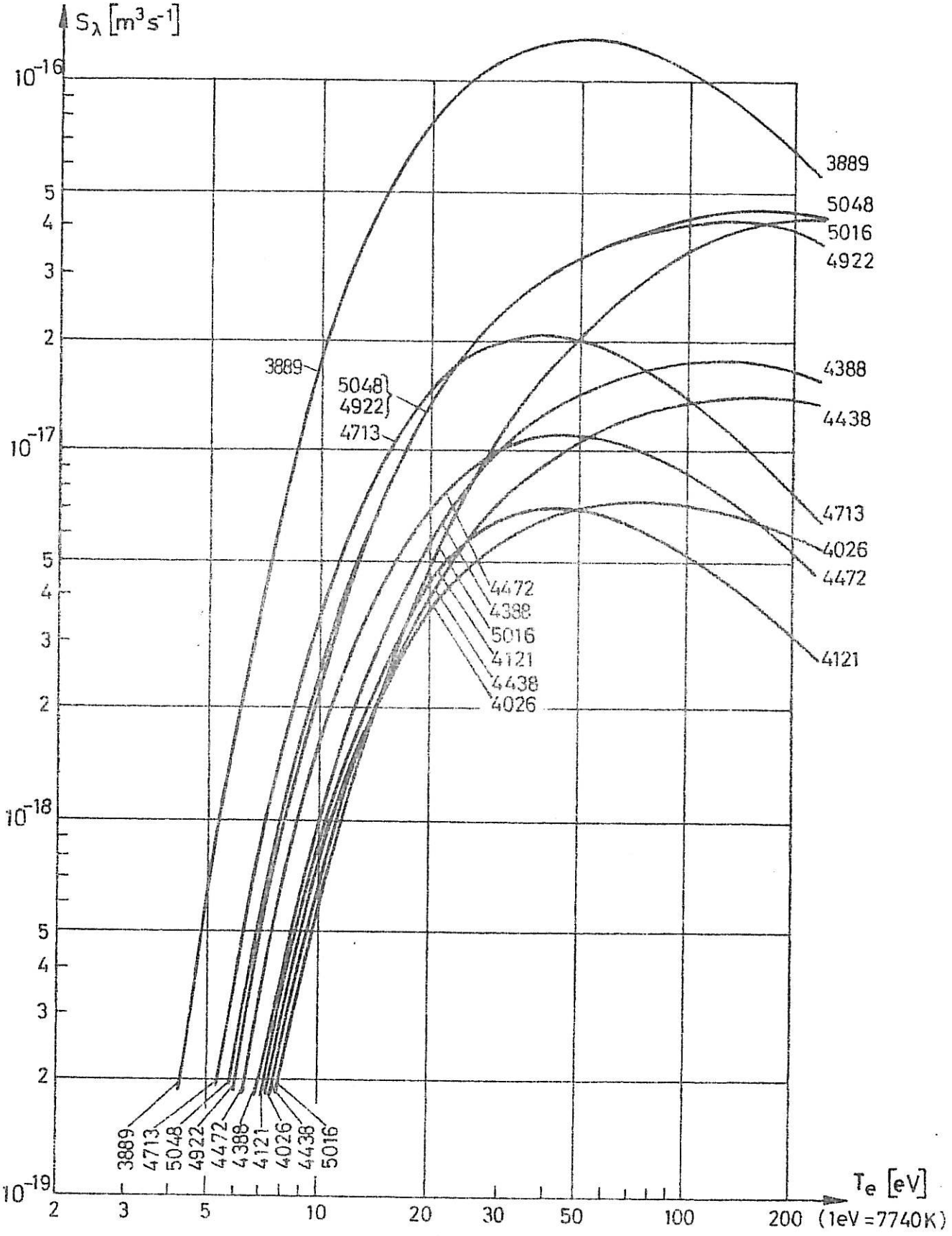

Fig. 5. Line excitation rates S_λ for ten He I lines (Appendix I.1.1).

TRITA-EPP-78-16

Royal Institute of Technology, Department of Plasma Physics,
S-100 44 Stockholm, Sweden

ELECTRON TEMPERATURE MEASUREMENTS IN LOW DENSITY PLASMAS BY HELIUM SPECTROSCOPY II - PARAMETER LIMITS FOR VALIDITY OF DIFFERENT METHODS

N. Brenning
December 1978, 44 pp. incl. illus., in English

Different methods to measure electron temperature in low-density plasmas by He spectroscopy are examined. They are based either on the relative intensities of singlet and triplet lines or on the absolute intensities of single lines. Calculations from measured and theoretical data show that both methods are seriously influenced by secondary processes, the dominating being excitation from the metastable levels 2^1S and 2^3S, and excitation transfer in electron-atom collisions combined with imprisonment of resonance radiation. The calculations give parameter limits for validity of different methods and combinations of lines. Due to the secondary processes, T_e-determination from relative line intensities is limited to low-density, short-duration plasmas (typically $n_e < 2 \cdot 10^{16} m^{-3}$, $t_{ex} < 5 \cdot 10^{-6} s$) or to even lower densities that depend on the apparatus dimensions (typically $n_e < 3 \cdot 10^{15} m^{-3}$, $L \approx 0.1$ m).

For T_e-determination from absolute line intensities the situation is more favourable, and with a suitable choise of lines the restrictions on n_e and t_{ex} can be typically ($n_e < 5 \cdot 10^{17} m^{-3}$, $t_{ex} < 10^{-5} s$) or ($n_e < 10^{17} m^{-3}$, $L \approx 0.1$ m) for electron temperatures above 10 eV. For temperatures below 10 eV and degrees of imprisonment below 7% measurements are possible for electron densities up to 10^{19} or $10^{20} m^{-3}$, and without any limits on t_{ex} or L.

Key words: Helium spectroscopy, Plasma diagnostics, Plasma spectroscopy.